

Original Paper

# Methylglyoxal Reshapes Hepatic and Adipose Tissue Metabolism and Increases Viability of Lymphocytes

Naiara Cristina Lucredi<sup>a</sup> Lucas Paulo J. Saavedra<sup>b</sup> Silvano Piovan<sup>b</sup> Emanuele P. Lima<sup>a</sup> Mariane Aparecida F. Godoy<sup>b</sup> Rogério Marchiosi<sup>a</sup> Verônica Elisa P. Vicentini<sup>b</sup> Paulo Cezar F. Mathias<sup>b</sup> Anacharis B. Sá-Nakanishi<sup>a</sup> Livia Bracht<sup>a</sup> Claudia C. S. Chini<sup>c</sup> Eduardo N. Chini<sup>c</sup> Adelar Bracht<sup>a</sup> Jurandir F. Comar<sup>a</sup>

<sup>a</sup>Department of Biochemistry, State University of Maringá, 87020900, PR, Brazil, <sup>b</sup>Department of Biotechnology, Genetics, and Cellular Biology, State University of Maringá, PR, Brazil, <sup>c</sup>Department of Anesthesiology and Perioperative Medicine, Mayo Clinic, Jacksonville, FL, USA

## Key Words

Methylglyoxal • Liver diseases • Advanced glycation end products • Gluconeogenesis • Liver metabolism • Inflammation

## Abstract

**Background/Aims:** Methylglyoxal (MG) is associated with the development of metabolic disorders that modify the hepatic energetic metabolism in different ways. However, not much is known about the effects of MG on energy metabolism in healthy liver cells. Therefore, this study investigated the effects of daily MG administration to Wistar rats on hepatic and fat tissue energetic metabolism. **Methods:** Rats received MG intraperitoneally at doses of 100 or 200 mg/kg for seven consecutive days in acute approach or at a dose of 25 mg/kg for one month in the chronic approach. Metabolic pathways were measured in isolated perfused livers (glycogen catabolism, gluconeogenesis and ketogenesis) as well in adipose tissue. Activities and mRNA expressions of gluconeogenic enzymes were assessed in the liver and the viability of human lymphocytes were evaluated *in vitro*. **Results:** MG displayed systemic inflammation and the metabolic changes were similar to those of widespread catabolic diseases. MG and advanced glycation end-products stimulated lymphocyte proliferation, and MG increased the hepatic interleukin-6 expression. Rats that received MG developed insulin resistance. Gluconeogenesis was diminished and glycolysis was stimulated in livers of rats that received MG. Two factors contribute to this outcome: a deficiency in mitochondrial energy supply and a much more significant downregulation of gluconeogenic enzymes. The adipose tissue metabolism was modified in a way that the AMPK-induced lipolysis was increased in the retroperitoneal fat, but not in the mesenteric fat. Ketogenesis was increased and triglycerides content was decreased in the liver. **Conclusion:** To what degree the modifications in hepatic

metabolism found in MG-exposed rats can be translated to patients with a high-grade inflammation and cirrhosis is uncertain. However, it is unlikely that the strong catabolic state induced by MG would not contribute in some way to the hepatic dysfunction in advanced liver diseases.

© 2025 The Author(s). Published by  
Cell Physiol Biochem Press GmbH&Co. KG

## Introduction

Methylglyoxal (MG) is a glycotoxin derived mainly from the trioses-phosphate (glycolytic intermediates). Increased intracellular levels of glucose or fructose drive the non-enzymatic production of MG and other  $\alpha$ -oxaldehydes via formation of Amadori products [1]. MG may also derive from lipids and proteins [2] and, once formed, promptly reacts with macromolecules, particularly proteins, to form advanced glycation end products (AGE) [1]. The main route of AGE generation is the reaction of MG with primary amines (N-terminal groups or side chain of lysine) or the guanidine group of arginine [3]. MG and AGE are known to deteriorate a variety of cell functions and are involved in the onset and progression of many metabolic disorders, such as obesity and diabetes [4]. In contrast, the glyoxalase system is the main route of MG detoxification, in which two enzymes, glyoxalases I and II, act in sequence to convert MG into lactate in a process dependent on reduced glutathione (GSH) [5].

The mechanisms by which MG and AGE cause deleterious effects involves structural modifications of intra- and extracellular proteins [4, 6]. Both MG and AGE modify collagen and other extracellular matrix proteins. Inside the cell, MG causes oxidative stress and modifies proteins involved in gene transcription. Extracellular AGE bind to AGE receptors (RAGE) and activate intracellular signaling pathways that lead to inflammation and oxidative stress. In turn, the RAGE expression is known to be upregulated by inflammatory cytokines and reactive oxygen species (ROS) through the activation of nuclear factor-kappa B (NF- $\kappa$ B) [7]. MG and AGE also downregulate the expression of glyoxalases in such metabolic disorders, a condition that leads to an even higher accumulation of these compounds [4].

Endogenous production is not the only source of MG and AGE because they are also formed in foods by Maillard reactions. Once absorbed from the digestive tract [8] they reach the liver, which is also the main site for their clearance [9]. Endogenous extrahepatic MG and AGE also reach the liver, contributing to an overloading that, under certain circumstances, substantially increases the chances of damage. Overloading of the liver also occurs in systemic diseases and is directly associated to the severity of the hepatic diseases [10, 11]. For example, the liver content of MG is increased in diabetic mice and in rats with CCl<sub>4</sub>-induced hepatitis [12, 13].

MG has been related to the onset and progression of many metabolic disorders that modify the hepatic energy metabolism in different ways, including modifications in opposite directions, i.e., stimulus of anabolic pathways in some diseases and catabolic ones in other conditions. MG is related to the progression of obesity, diabetes and MASLD, all of these linked to stimulation of hepatic anabolic pathways, such as gluconeogenesis and lipid synthesis [14]. In contrast, MG is also related to the development of steatohepatitis and cirrhosis, which are linked to stimulation of catabolic pathways in the liver and systemically [15]. The latter are associated with reduction of hepatic gluconeogenesis and glycogen stores, stimulus of lipolysis, anorexia and cachexia [15, 16]. In this regard, high circulating levels of MG are associated with advanced cirrhosis and systemic inflammation [17]. In fact, high-grade inflammation has been reported to be the major driver of cirrhosis and liver failure [18]. In addition, high-grade systemic inflammation is related to a widespread catabolism in the body, including stimulus of catabolic pathways in the liver [19-21].

Although the role of MG in chronic liver disease has been extensively investigated, not much has yet been done to clarify the effects of this glycotoxin on energy metabolism in healthy liver cells. Investigations of this kind can help to distinguish between the metabolic modifications that are elicited by disease and those ones caused solely by MG. To fill this

gap was the purpose of the present work. MG was intraperitoneally administered to rats and metabolic pathways were measured in the isolated perfused liver (glycogen catabolism, gluconeogenesis and ketogenesis) as well in adipose tissue. It was in addition evaluated the respiratory activity in isolated hepatic mitochondria and the influence of MG and AGE on the viability of lymphocytes. Additional mechanistic insights were gained by measuring enzyme activities, mRNA expression of key enzymes, cytokines and RAGE and the contents of AGE, MG and oxidative state markers.

## Materials and Methods

### *Materials*

Methylglyoxal (MG), bovine serum albumin (BSA), enzymes and coenzymes were purchased from Sigma Chemical Co (St. Louis, MO, USA). Anti-phospho-AMPK and anti-AMPK antibodies were purchased from Cell Signaling Technology® (Danvers, MA, USA). Anti-β-actin antibody was purchased from Santa Cruz Biotechnology (Santa Cruz, CA, USA). Anti-carboxymethyllysine and anti-methylglyoxal antibodies were purchased from Abcam (Cambridge, UK). Chemiluminescence Amersham™ ECL Prime reagent was purchased from GE Healthcare (Chicago, IL, USA). Trizol™ reagent and QuantiNova® Reverse Transcription Kit was purchased from Thermo Fisher Scientific (Waltham, MA, USA). Commercial kits for AST, ALT, albumin, total protein, glucose, triglycerides (TAG), total cholesterol (CHOL) and HDL CHOL were purchased from Gold Analisa Diagnóstica Ltda (Belo Horizonte, MG, Brazil). The ELISA kit for MG assay was purchased from ELK Biotechnology Co (Denver, CO, USA).

### *Animal housing and experimental design*

Male *Wistar* rats weighing 180-220g (50 days old) were obtained from the Central Animal Facility of the State University of Maringá (UEM). The animals were housed in polypropylene cages (four animals per cage) under controlled temperature ( $24 \pm 3$  °C) with 12-hour light/dark lighting cycles and free access to standard diet (Nuvilab®, Colombo, PR, Brazil) and water. All procedures were performed as recommended by the Brazilian National Council for the Control of Animal Experiments (CONCEA) and were approved by the Ethics Commission in for the Use of Animals (CEUA) of UEM (Protocol Number 9185221019).

In the acute approach, animals were randomly distributed into three groups (n = 7 per group): control rats (Co), which received 5 mL/kg of 0.9% saline; rats MG100 and MG200, which received 100 and 200 mg/kg MG, respectively. MG (or saline) was administered through intraperitoneal injection for seven consecutive days. In the chronic approach, animals received saline (vehicle) or 25 mg/kg MG by intraperitoneal injection for one month. The chronic approach was carried out to evaluate the effects of long-term exposure to MG. Body weight and food consumption were monitored every 2 days. The doses and frequency of administration for MG were based on previous studies [22-25] and they are required to maintain a stabilized MG concentration in the plasma at approximately three times greater than the baseline [25]. Such MG levels align with those found in pathological conditions [1, 2,17].

### *Evaluation of glucose homeostasis*

Glycemic homeostasis was evaluated by measuring fasting blood glucose levels, and by performing oral glucose tolerance tests (OGTT) and insulin tolerance tests (ITT). OGTT was performed by oral administration (gavage) of glucose (1.5 g/kg) to 12 h fasted rats. At appropriate times, blood samples were taken after tail incision and glucose was measured using a glucometer (AccuChek Active®, Roche). Fasting glycemia corresponds to the blood glucose levels just before glucose administration. The ITT was performed by an intraperitoneal injection of regular insulin (1 U/kg) in rats fasted for 12 h followed by blood glucose measurements at times 0, 5, 10, 15, 20, 25 and 30 min. The  $k_{ITT}$  values were calculated as the slopes of the linear segment of the ITT curves.

### *Tissue collection and processing*

Rats fasted for 12 h were deeply anesthetized by intraperitoneal injection of a combination of xylazine (9 mg/kg) and ketamine (90 mg/kg). Afterwards the peritoneal cavity was exposed and blood was collected from the cava vein for obtaining the plasma fraction. Next, the liver was removed and divided into two

portions: one was processed for evaluation of proteins expression, enzymes activities and subcellular organelles isolation. The other liver portion was immediately frozen in liquid nitrogen for assessment of hepatic lipids, MG and oxidative stress. Finally, the retroperitoneal, periepididymal and mesenteric white fat depot and the gastrocnemius and soleus muscles were removed and weighed. Subsequently, fat depots were snap frozen for western blot analysis.

For assessment of lipids and oxidative stress, the frozen portion of tissue was homogenized in a Van Potter-Elvehjem homogenizer with 10 volumes of ice-cold 0.1 M potassium phosphate buffer (pH 7.4). An aliquot was separated for use as total homogenate, and the remaining portion was centrifuged at 11, 000g by 15 min. The supernatant separated as a soluble fraction of the homogenate. For assessment of MG, liver was homogenized in ice-cold PBS (PBS; pH 7.4) and centrifuged at 10, 000g for 10 min. The supernatant was collected and used to MG determination by ELISA.

### *Adipocytes isolation and analysis*

Adipocytes from the retroperitoneal, periepididymal and mesenteric fat pads were isolated as previously described [26]. Briefly, adipose tissue was removed, minced with scissors, the fragments placed in a digestive buffer (pH 7.4) containing collagenase II and incubated at 37°C for 60 min under gentle agitation. The digested tissue was filtered, washed with Earle/Hepes buffer (EHB; pH 7.4) and the cells resuspended in this medium. After resting for 30 min, the infranatant was aspirated and the decanted adipocytes resuspended with paraformaldehyde for morphometric analysis. Images were captured by optical microscopy (Nikon Eclipse E110®, Tokyo, Japan) at 20x magnification. Five images per animal were captured and the area of 10 adipocytes per image was measured, resulting in 50 adipocytes/animal. The areas of adipocytes were determined using the ImageJ® software (National Institute of Health – NIH).

### *Plasma analytical assays*

The levels of total and HDL CHOL, TAG, total protein, albumin, MG and AST and ALT activities were determined in the plasma using commercial kits. The myeloperoxidase (MPO) activity was determined by spectrophotometry (460 nm) with o-dianisidine [27]. The levels of glycerol were determined by spectrofluorimetry ( $\lambda_{\text{ex}} = 350$  nm and  $\lambda_{\text{em}} = 465$  nm) using glycerol dehydrogenase [28]. This method relies on the fluorescence of NADH formed from NAD<sup>+</sup> when glycerol is oxidized to dihydroxyacetone in the reaction catalyzed by glycerol dehydrogenase. The levels of  $\beta$ -hydroxybutyrate and acetoacetate were quantified by spectrophotometry using  $\beta$ -hydroxybutyrate dehydrogenase (340 nm) [29]. Maillard compounds (AGE levels) were assayed by spectrofluorimetry ( $\lambda_{\text{ex}} = 370$  nm and  $\lambda_{\text{em}} = 440$  nm) [30].

### *Oxidative stress parameters*

Oxidative stress was assessed in the plasma and liver. The ferric reduction capacity of plasma (FRAP) was determined by spectrophotometry (593 nm) [31]. Total antioxidant capacity (TAC) of the plasma was assayed by colorimetric method using 2, 2'-azinobis (3-ethylbenzothiazoline-6-sulfonic acid) or ABTS [32]. The content of protein sulfhydryl groups (thiols) was determined in plasma by spectrophotometry (412 nm) using 5,5'-dithiobis(2-nitrobenzoic acid) (DTNB) [32]. The levels of protein carbonyl groups were determined in plasma and supernatant of liver homogenate by spectrophotometry with 2, 4-dinitrophenylhydrazine (DNPH) [33]. The contents of reduced (GSH) and oxidized (GSSG) glutathione were determined in the liver homogenate by spectrofluorimetry ( $\lambda_{\text{ex}} = 350$  nm and  $\lambda_{\text{em}} = 420$  nm) with o-phthalaldehyde (OPT) [34]. Reactive oxygen species (ROS) was quantified in the supernatant of homogenate by spectrofluorimetry ( $\lambda_{\text{ex}} = 504$  nm and  $\lambda_{\text{em}} = 529$  nm) using 2, 7-dichlorofluorescein diacetate (DCFH-DA) [35]. The catalase activity was estimated in the supernatant of liver homogenate by measuring changes in absorbance at 240 nm using H<sub>2</sub>O<sub>2</sub> as substrate [29]. The activity of superoxide dismutase (SOD) was estimated spectrophotometrically (420 nm) by its ability to inhibit the pyrogallol autoxidation in alkaline medium [36]. The expression in terms of mRNA of catalase, glutathione reductase (GR), glutathione S-transferase alpha 3 (GSTA3), glutathione peroxidase-1 (GPx1) and heme oxygenase 1 (HO-1) were determined by RT-PCR.

### *Hepatic lipids and AGE content*

Total lipids were extracted from frozen livers with a chloroform-methanol mixture (2:1) and quantified by a gravimetric method [20]. The extracted lipids were dissolved in a chloroform-isopropanol mixture (1:2) for quantifying TAG and CHOL using commercial kits. AGE levels were quantified in the liver homogenate,

which was centrifuged at 16, 000g for 1 hour. The supernatant was separated, diluted 10×, and Maillard compounds were assayed in the same way as in plasma [30].

### *Liver perfusion and metabolism*

Hemoglobin-free non-recirculating liver perfusion was performed as earlier described [37]. Rats were deeply anesthetized by an intraperitoneal injection of xylazine (9 mg/kg) plus ketamine (90 mg/kg) and the peritoneal cavity was exposed by laparotomy. After cannulation of the portal and cava veins, the liver was removed and positioned in a plexiglass chamber. The perfusion fluid was Krebs/Henseleit-bicarbonate buffer (pH 7.4) containing 25 mg% BSA and saturated with a mixture of oxygen and carbon dioxide (95:5) by means of a membrane oxygenator with simultaneous temperature adjustment at 37 °C. The flow was maintained constant by a peristaltic pump (Minipuls 3, Gilson, France). Oxygen concentration in the venous perfusate was monitored by a teflon-shielded platinum electrode. Samples of the venous perfusate were collected at two minutes intervals and analyzed for their metabolites contents.

Glycolysis and glycogenolysis were measured in livers isolated from fed rats, which were perfused with the perfusion fluid in the absence of exogenous substrates [38]. Glucose, lactate and pyruvate were assayed in the effluent perfusate by standard enzymatic procedures [29]. Glucose was measured by spectrophotometry (505 nm) using the enzymatic-colorimetric glucose oxidase method. Lactate and pyruvate were assayed by spectrophotometry using the lactate dehydrogenase reaction. At the steady-state, glycolysis was defined as  $(\text{lactate} + \text{pyruvate})/2$  and glycogenolysis =  $\text{glucose} + [(\text{lactate} + \text{pyruvate})/2]$ .

Gluconeogenesis was measured in the livers of 12 h fasted rats and L-lactate (2 mM) or D-glycerol (5 mM) was infused as a glucose precursor [39]. The livers were initially perfused with Krebs/Henseleit buffer in the absence of exogenous substrates. After stabilization of oxygen consumption, L-lactate (2 mM) or glycerol (5 mM) was added to the perfusion fluid by 30 min. Glucose, lactate and pyruvate were assayed in the effluent perfusate [29].

Ketogenesis was measured in the livers of 12 h fasted rats and palmitic acid (0.3 mM) was used as substrate [40]. Acetoacetate and  $\beta$ -hydroxybutyrate were assayed in the effluent perfusate [29].

### *Liver mitochondria and microsomes isolation*

Fresh livers were placed in a medium containing 200 mM mannitol, 75 mM sucrose, 0.2 mM ethylene glycol tetraacetic acid (EGTA), 2 mM Tris-HCl, pH 7.4 and 50 mg/dL BSA. The organ was minced, washed and homogenized in the same medium with a Van Potter-Elvehjem homogenizer. Hepatic mitochondria and microsomes were isolated by differential centrifugation: 600g (10 min) and 7, 000g (10 min) for mitochondria [41]; the supernatant was then centrifuged at 12, 400g (10 min), the supernatant was collected and centrifuged again at 105, 000g (60 min). The resulting pellet was the microsomal fraction [42].

### *Mitochondria respiration and membrane potential (MMP)*

Mitochondrial oxygen consumption was measured by polarography using a teflon-shielded platinum electrode as earlier described [43]. Isolated mitochondria were incubated in the closed oxygraph chamber with the respiration medium (2.0 mL). The substrates were 10 mM succinate or  $\alpha$ -ketoglutarate. Rates of oxygen consumption were computed from the slopes of the recorder tracings. The respiration rates were measured under three conditions: Before the addition of ADP (basal respiration), just after 0.125 mM ADP addition (state III respiration) and after cessation of the ADP stimulation (state IV). The respiratory control (RC) was the ratio of state III/state IV and the ADP/O ratio was calculated as earlier described [44].

Freeze-thawing disrupted mitochondria were used to measure the activities of succinate-oxidase and NADH-oxidase by polarography. Disrupted mitochondria were incubated in the respiration medium (20 mM Tris-HCl, pH 7, 4) and the reaction was started by the addition of substrates, 1 mM NADH and 1 mM succinate, for NADH-oxidase and succinate-oxidase, respectively. The couple TMPD-ascorbate was in addition used as electron donating substrate to cytochrome c/complex IV of the mitochondrial respiratory chain.

MMP was measured by spectrofluorimetry ( $\lambda_{\text{ex}} = 520 \text{ nm}$  and  $\lambda_{\text{em}} = 580 \text{ nm}$ ) using the dye safranin [45]. Mitochondria (1 mg protein) were incubated in a medium (2mL) containing 0.25 M mannitol, 5 mM potassium phosphate, 10 mM Tris (pH 7.4), 0.2 mM EGTA, 50 mg% BSA and 10 $\mu$ M safranin. The latter accumulates in polarized mitochondria. The energization was achieved with 50  $\mu$ M succinate and after, the complete depolarization was achieved with 10  $\mu$ M carbonyl cyanide 4-(trifluoromethoxy)phenylhydrazone (FCCP). The MMP was calculated by subtracting the fluorescence obtained with FCCP from that one obtained

with succinate and expressed as arbitrary fluorescence units (AFU).

### *Hepatic gluconeogenic enzymes activity*

The activity of glucose 6-phosphatase (G6Pase) was measured in isolated microsomes by the spectrophotometric quantification of the released phosphate from glucose 6-phosphate [42]. The activities of fructose 1, 6-bisphosphatase (FBPase-1) and phosphoenolpyruvate carboxykinase (PEPCK), glycerol-3-phosphate dehydrogenase (GPDH) and glycerol kinase (GK) were determined using the supernatant of the centrifugation at 105,000g that was obtained in the procedure of microsomes isolation (Section 2.10). The FBPase-1 activity was measured by the spectrophotometric quantification of the released phosphate from fructose-1, 6-bisphosphate [40]. The PEPCK activity was estimated by coupling the malate dehydrogenase to the PEPCK reaction [40]. The NADH oxidation by oxaloacetate formed in the PEPCK reaction was assayed by spectrophotometry (340 nm). The GK activity was performed with a coupled assay with GPDH and GPDH activity was assayed by spectrophotometry following the NADH oxidation at 340 nm [29].

### *Western Blot*

Fresh livers (50mg) or adipose tissues (100mg) were homogenized in a lysis buffer (100 mM Tris/HCl, pH 7.5, 100 mM sodium pyrophosphate, 100 mM sodium fluoride, 100 mM sodium orthovanadate, 2 mM PMSF, and aprotinin 1mg/mL) and centrifuged at 12,000g for 20 min. The pellet was discarded and the supernatant used for the procedure. Total protein was determined as earlier [46]. Aliquots of supernatant (30 µg protein) were added to Laemmli buffer, heated at 100 °C for 5 min, applied on 10% SDS-PAGE and transferred to a nitrocellulose membrane overnight (20 V). The membranes were then submitted to blocking buffer, and subsequently incubated overnight at 4 °C with primary antibodies (anti-phospho-AMPK, anti-AMPK and anti-β-actin). Membranes were washed, incubated with horseradish peroxidase-conjugated secondary antibody and covered with chemiluminescence detection Amersham ECL Prime reagent. The bands were visualized using the ImageQuant LAS 500 (GE Healthcare Life Sciences, Chicago, IL, USA) and intensities were analyzed using ImageJ software (National Institute of Health, Maryland, USA).

### *Dot blot*

A liver sample (50 mg) was homogenized with lysis buffer, centrifuged at 12,000g for 20 min, the pellet discarded and the protein content measured in the supernatant [46]. Aliquots of supernatant were added at the final concentration of 3 µg/µL to Laemmli buffer, heated at 100 °C for 5 min and 3µL applied to an activated PVDF (polyvinylidene difluoride) membrane. The dots were left to dry overnight and the membrane was thereafter reactivated with methanol and stained with 0.025% coomassie blue R-250 in 40% methanol and 7% acetic acid. The stained membrane was washed 3 times with a destain solution composed by 50% methanol and 7% acetic acid (v/v). The coomassie blue stain was detected using ImageQuant LAS 500 (GE Healthcare Life Sciences, Chicago, IL, USA) and used as a loading control. Coomassie blue was thereafter completely removed with pure methanol from the membrane, which was washed in TBS-T solution and incubated in TBS-T blocking reagent. The membranes were then incubated overnight at 4 °C with primary antibodies: anti-methylglyoxal (anti-MG) diluted 1:1000 or anti-carboxymethyllysine (anti-CML) diluted 1:2000 and in the next day with a secondary antibody anti-mouse diluted 1:5000. Membranes were gently washed, incubated with horseradish peroxidase-conjugated secondary antibody and covered with chemiluminescence detection Amersham ECL Prime reagent. The bands were visualized using the ImageQuant LAS 500 and the intensities were analyzed using the same ImageJ software.

### *RNA isolation and real-time quantitative RT-qPCR*

Liver samples were collected and stored in liquid nitrogen for total RNA extraction. RNA was isolated from 100 mg frozen tissue using Trizol reagent. The RNA concentration was measured by spectrophotometry at 260 nm (NanoDrop ND 1000 NanoDrop Technologies, Wilmington, DE). The integrity of RNA (RNA integrity number - RIN) was evaluated in Bioanalyzer RNA 6000 (Agilent, USA). cDNA was synthesized using the QuantiNova® Reverse Transcription Kit and the quantitation of the tissue expression of selected genes was done by quantitative PCR in a Rotor-Gene® Q (Qiagen) with "HOT FirePol® EvaGreen® qPCR Supermix" (Solis BioDyne, EE). The GAPDH gene was utilized as reference. The 2-ΔCT method was used for the relative quantification analysis and data were expressed in arbitrary units (AU). Primer sequences of all genes are presented as Supplemental Material (Table S1).

#### *Volunteers, human lymphocytes isolation and primary lymphocyte culture*

Venous blood was collected from four healthy male volunteers aged between 20 and 30 years, non-smoker, with no historical of chronic diseases and who did not use prescription drugs. The procedure was performed in accordance with the Code of Ethics of the World Medical Association (Declaration of Helsinki) and approved by the Human Ethics Committee of the State University of Maringá (Application n° 70612823.1.0000.0104). Blood was collected using a 20mL heparinized disposable syringe. Peripheral lymphocytes were isolated as previously described [47], with modifications. Blood was distributed in Falcon tubes and diluted in a 1:1 ratio with sterile 0.85% saline. After another dilution with Ficoll Paque Plus (1:3 v/v), the tubes were centrifuged at 1500 rpm for 30 min to separate blood into plasma, red cells and white cells. The buffy coat (leukocytes) was collected, diluted in Hanks solution (3:1) and centrifuged at 1100 rpm for 10 minutes. The supernatant was discarded and the procedure repeated once more to wash the cells. Next, the cell pellet was resuspended in 1mL of RPMI medium supplemented with 20% FBS (Gibco) and 2% phytohemagglutinin A (Gibco), and the cells were counted in a Neubauer chamber. Lymphocyte cultures were grown in 96-well plates containing RPMI medium supplemented with phytohemagglutinin A and SBF, in an oven at 37°C and humidified atmosphere.

#### *AGE preparation and lymphocytes viability assay*

AGEs were obtained by incubating 50 mg/mL albumin (BSA) with 50 mM MG (AGE-L) or 250 mM MG (AGE-H) in 1 M sodium phosphate buffer (pH 7.4) at 50 °C for 4 days under sterile conditions. After this period, the solutions were filtered (0.22 µm) and dialyzed against 0.1 M PBS, pH 7.4 at 4 °C for 24 h [48]. Next, the solution was again filtered, aliquoted and stored at -80°C. The AGE preparations were characterized in relation to non-oxidized amino acids, Maillard compounds, protein carbonyl and sulphydryl groups, N-oxidized of amino acids, and contents of carboxymethyllysine (CML) and methylglyoxal-hydroimidazolone 1 (MG-H1). The results of AGE characterization are presented as Supplementary material (Fig. S1).

The viability of human lymphocytes was evaluated using the MTT (3-(4, 5-dimethylthiazol-2-yl)-2, 5-diphenyltetrazolium bromide) assay, on the basis of the cellular conversion of tetrazolium salt into formazan. Cells were seeded at a density of 10<sup>6</sup> cells per mL in 96-well plates and allowed to grow for 24 or 48 h at 37 °C in the presence of AGE-L or AGE-H at the concentrations of 0.1, 1 and 2.5 mg/mL. Such AGE concentrations were based on a previous study [48]. Additional groups of lymphocytes were incubated under the same conditions with MG at concentrations in the range of 5-2000 µM. Following this incubation period, cells were washed with PBS and incubated with MTT (0.5 mg/mL) for 2 h. The MTT medium solution was removed, formazan crystals were solubilized by adding DMSO (100 µL/well) and the absorbance of the solution was measured at 550 nm. Five independent experiments were conducted, and the results are presented as percentage of controls, to which 100% activity was attributed [49].

#### *Statistical analysis*

Results are expressed as mean ± standard error of the mean (SEM). Statistical analysis was done using GraphPad Prism Software (version 8.0). For three or more values, the statistical significance of the data was analyzed by means of ANOVA ONE-WAY, and a Newman Keuls *posthoc* test was applied with the 5% level ( $p < 0.05$ ). For the comparison of two values, the student *t-test* was applied with the 5% and 1% level ( $p < 0.05$  and  $p < 0.01$ ).

## Results

#### *MG impairs the body weight gain and decreases the food intake*

In order to evaluate if MG administration affects the body weight and food intake, these parameters were monitored every 2 days. The results are shown in Fig. 1. The body weight gain was diminished by the MG administration in a dose-dependent manner over the entire seven-day treatment period (Fig. 1A). After 7 days, the weight of the rats that received 100 and 200 mg/kg was 40% and 56% lower, respectively, compared to the controls (Fig. 1B). The daily food intake was lower in the group that received 100 mg/kg MG and even lower in

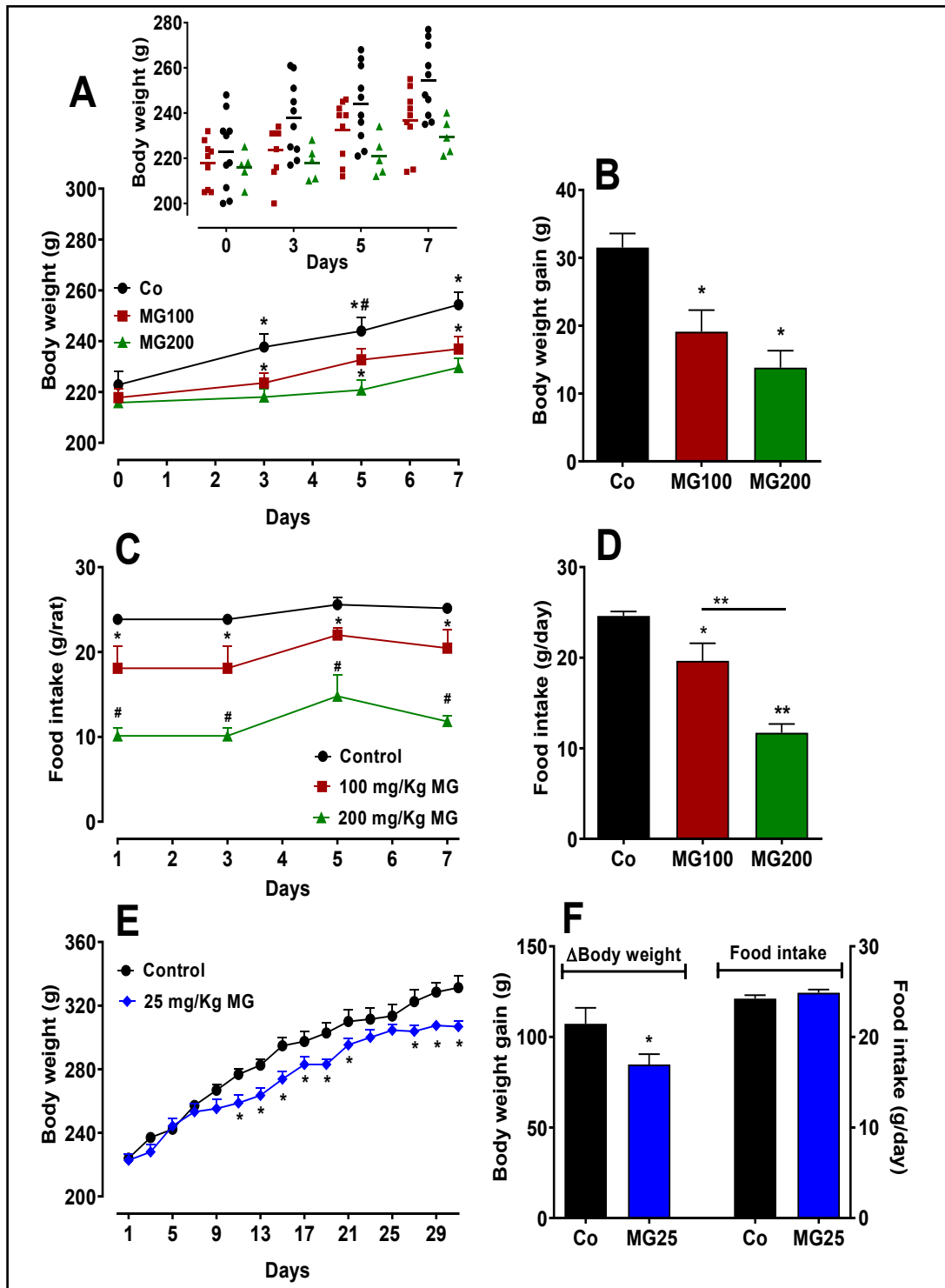


**Fig. 1.** Effects of methylglyoxal (MG) on body weight and food intake of rats. The animals received daily i.p. saline (Co; Control), 100 mg/kg (MG100) or 200 mg/kg (MG200) MG for 7 days or 25 mg/kg MG (MG25) for one month. A: Evolution of body weight during 7 days. The insert in Panel A shows the individual body weights as a scatter plot. B: Body weight gain during 7 days. C: Daily food intake evolution during 7 days. D: Daily food intake average of 7 days. E: Evolution of body weight for one month. F: Body weight gain in one month and daily food intake mean of one month. Values are the mean  $\pm$  SEM of 6-8 animals. \* $p < 0.05$  and \*\* $p < 0.0001$ : different from Co; # $p < 0.05$ : difference between MG100 and MG200.

the group that received 200 mg/kg MG (Fig. 1C). The average daily food intake over a week was 20% and 52% lower in the groups that received 100 and 200 mg/kg MG, respectively (Fig. 1D). Rats that received MG at the lower dose of 25 mg/kg during one month (MG25), also slowed down weight gain when compared to the controls, but the phenomenon was much less pronounced and occurred only from the 10<sup>th</sup> day on (Fig. 1E). After a month of exposure to 25 mg/kg MG, a 20% reduction in body weight was observed when compared to the controls (Fig. 1F). The daily food intake for the group that received 25 mg/kg MG during the treatment period was not different from that of the controls (Fig. 1F). The last observation suggests that reduction in food intake may not be the sole cause of the reduction in weight gain caused by the glycotoxin.

#### *MG modifies the pattern of body fat deposition and causes loss of lean mass*

Given that MG affected body weight gain, body composition in terms of fat and muscle mass was analysed. These results and the areas of the adipocytes are shown in Fig. 2. MG at the dose of 100 mg/kg did not modify the weight of periepididymal and retroperitoneal fat, but at the dose of 200 mg/kg it decreased the weight of both fats by 32% and 56%, respectively (Fig. 2A). On the other hand, MG (100 and 200 mg/kg) increased the weight of mesenteric fat by 75%. The administration of 25 mg/kg MG for one month did not modify the weight of the adipose tissues (Fig. 2B). MG at the doses of 100 and 200 mg/kg decreased the gastrocnemius muscle weight by 6% and 20%, respectively (Fig. 2C). Only 200 mg/kg MG decreased the weight of the soleus muscle (-22%). The administration of 25 mg/kg MG for one month did not modify the weight of the muscles (Fig. 2C). In order to clarify the different profiles of the fat pads, the adipocytes were isolated from these depots, and their size was analysed. Fig. 2E shows representative optical microscopy images of adipocytes isolated from each of the three adipose tissues obtained from the groups that receive saline (control), 100 mg/kg (MG100) and 200 mg/kg MG (MG200). The adipocytes areas obtained from these images are shown in Fig. 2D. In the adipocytes from the retroperitoneal fat, both doses, 100 and 200 mg/kg, decreased their areas by 17% and 45%, respectively (Fig. 2D). Only the 200 mg/kg dose modified the area of the adipocytes from periepididymal fat (-28%). Finally, the areas of the adipocytes from mesenteric fat were increased by 86% and 22% by the doses of 100 and 200 mg/kg, respectively. Muscle loss evidences a more accelerated catabolic state in animals that received MG, while the loss of the periepididymal and retroperitoneal adipose mass is associated with the reduction in the area of adipocytes. However, adipocytes from mesenteric adipose mass exhibited hypertrophy. Together, these finds show that the administration of MG promoted a redistribution of fatty tissue without changing the total fat mass.

#### *MG decreases gluconeogenesis and downregulates key enzymes in the liver*

In order to evaluate if a catabolic state is present in the liver, the next step was investigating the effects of MG on hepatic pathways involved in energy metabolism. The effect of MG on gluconeogenesis was investigated in perfused livers using firstly lactate as a precursor. This compound is one of the main gluconeogenic substrates in humans and rodents and in addition allows the evaluation of the complete gluconeogenic machinery from pyruvate up to glucose [38, 39]. Fig. 3A shows the time courses of glucose and pyruvate production and oxygen uptake in perfused livers. These results refer to rats which received saline (Co), 100 mg/kg MG (MG100) or 200 mg/kg (MG200) for 7 days and also to rats which received 25 mg/kg MG (MG25) for one month. The results of controls (Co) which received saline for 7 days or one month were not substantially different and were omitted from Fig. 3A. As noted, the basal rates of glucose and pyruvate production were minimal and similar for all groups. The basal rates of oxygen uptake were lower in the liver of rats which received MG. After the onset of lactate infusion glucose and pyruvate production and oxygen consumption were differently stimulated in livers of controls and rats which received MG. Fig. 2B, C and D allow comparing the increments in each parameter upon 2 mM lactate infusion. Compared to the controls the increment in glucose production, corresponding to gluconeogenesis,

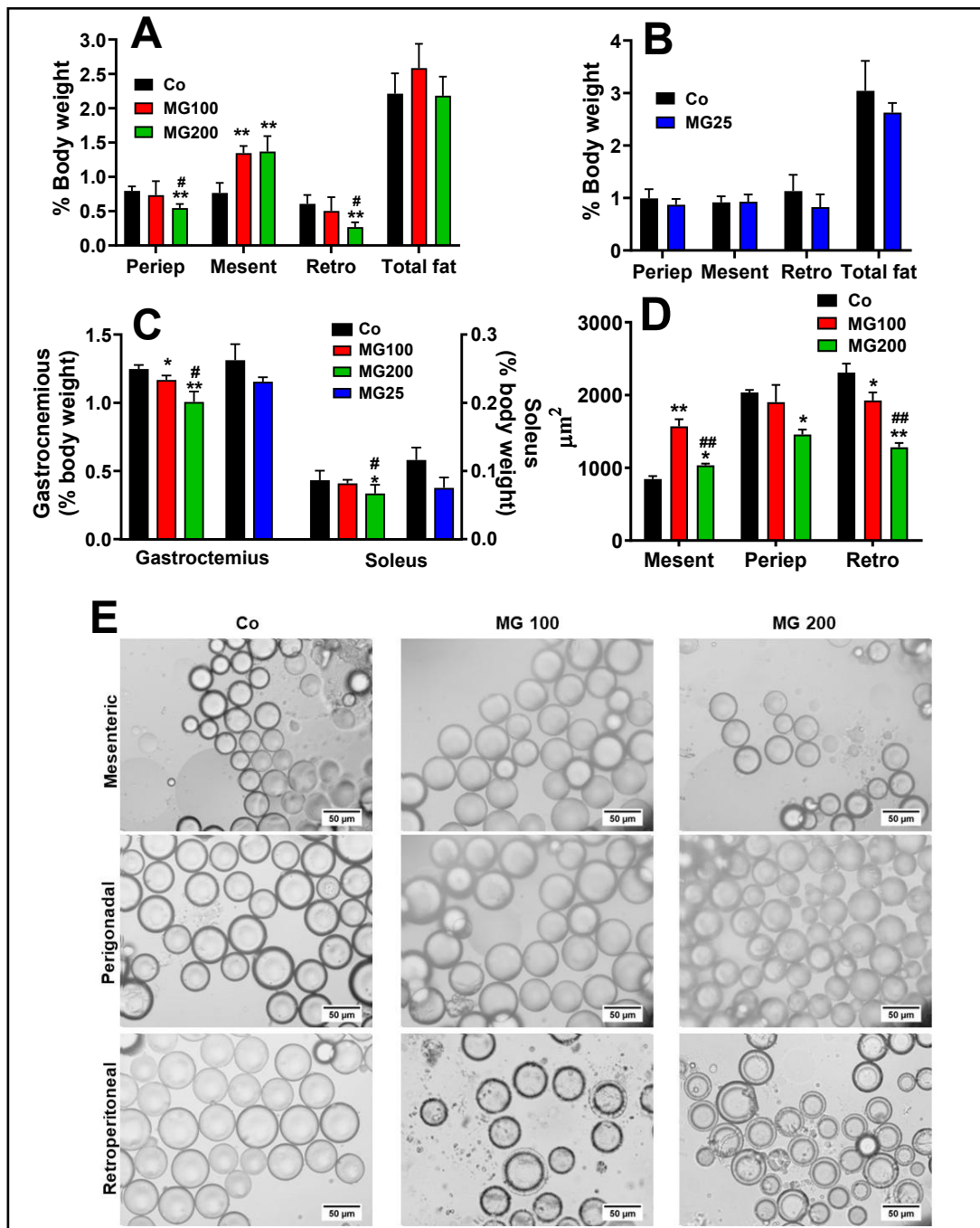


**Fig. 2.** Biometric parameters and morphometric analysis of adipocytes. The animals received i.p. saline (Co), 100 or 200 mg/kg MG (MG100 and MG200) for 7 days or 25 mg/kg MG (MG25) for one month. A and B: Adipose tissues weight of rats that received MG for 7 days and one month, respectively. C: Muscles weight. D: Adipocytes area in  $\mu\text{m}^2$ . E: Optical photomicrographs of adipocytes isolated from retroperitoneal (Retro), mesenteric (Mesent) and periepididymal (Periep) adipose tissues. Tissues weights are expressed as % of body weight and they are mean  $\pm$  SEM of 4-8 animals. \* $p < 0.05$  and \*\* $p < 0.0001$ : different from Co; # $p < 0.05$  and ## $p < 0.0001$ : difference between MG100 and MG200.

was approximately 40% lower in livers from rats that received 100 mg/kg and 200 mg/kg MG and 22% lower in livers from rats that received 25 mg/kg MG. The response of oxygen uptake was depressed by approximately 34% only in the group that received 25 mg/kg MG. Pyruvate production (Fig. 2D) from lactate was increased (65%) only in livers from rats that received 200 mg/kg MG.

The effects of 25 mg/kg MG on biometric parameters and hepatic gluconeogenesis were in general lower (or even absent) than those of 100 and 200 mg/kg MG. For this reason, the subsequent evaluations were carried out only with 100 and 200 mg/kg MG. Considering that MG impaired the gluconeogenesis, we investigated the contribution of the gluconeogenic rate-limiting enzymes for this phenomenon. The activity of PEPCK and FBPase-1 were, respectively, 58% and 45% lower in livers from rats that received 100 and 200 mg/kg MG (Fig. 3E and F). The activity of G6Pase was 18% and 38% lower, respectively, in the groups that received 100 and 200 mg/kg MG (Fig. 3G). The hepatic mRNA expressions of PEPCK and FBPase-1 were, respectively, 41% and 48% diminished in the animals which received 200 mg/kg MG (Fig. 3E and F). The hepatic mRNA expression of G6Pase was 140% increase in the liver from rats that received 200 mg/kg MG (Fig. 3G).

The effect of MG on gluconeogenesis was also investigated in perfused livers using glycerol as glucose precursor. Glycerol enters in an upper point of the gluconeogenic pathway and it needs only a third of the energy required to synthesize glucose from lactate. The reaction of glycerol kinase is the only step that requires ATP for the synthesis of glucose from glycerol. The use of glycerol as precursor allows inferring if the inhibition of gluconeogenesis occurs in an upper or lower point of the pathway. In addition, glycerol in the liver undergoes

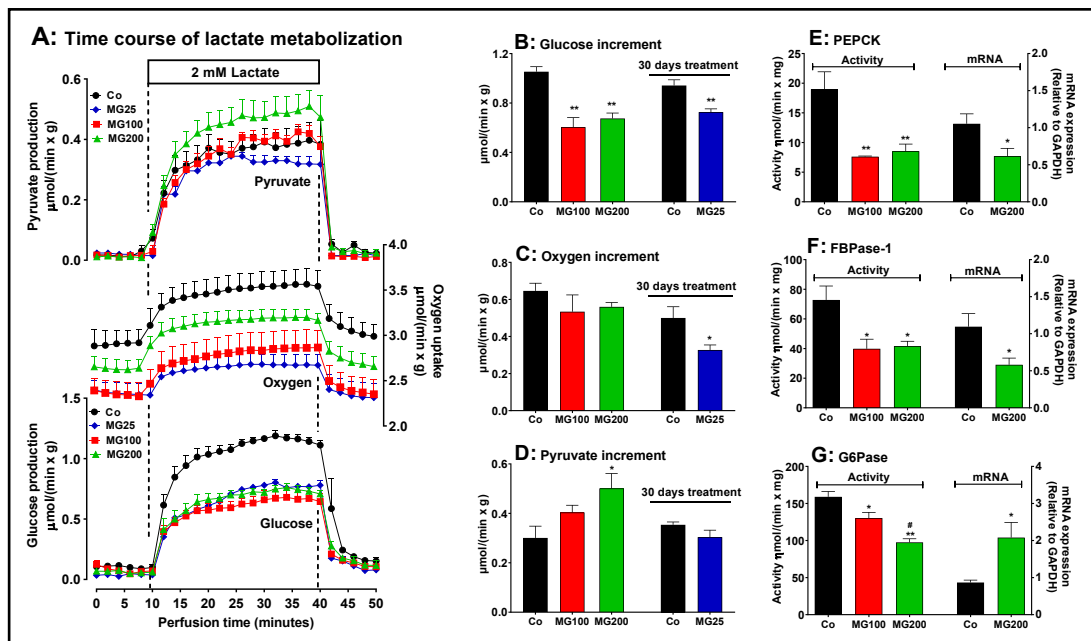


**Fig. 3.** Effects of MG on hepatic gluconeogenesis from lactate and activities and mRNA expressions of key gluconeogenic enzymes. Panel A: time courses of glucose and pyruvate production and oxygen consumption due to lactate infusion. The animals received i.p. saline (Co), 100 or 200 mg/kg MG (MG100 and MG200) for 7 days or 25 mg/kg MG (MG25) for one month. Livers from 12 h fasted rats were perfused with Krebs/Henseleit-bicarbonate buffer in combination with 2 mM L-lactate as indicated by the horizontal box in Panel A. The outflowing perfusate was sampled at regular intervals and analyzed for its contents of glucose, lactate and pyruvate. Oxygen uptake was monitored by polarography. The values in Panels B, C and D are the increments of metabolites production due to lactate infusion. They were calculated from the data in Fig. 3A as [final values at the end of the infusion period with L-lactate; 28 min] - [basal rates before infusion of L-lactate; 8 min]. Panels E, F and G show the effects of MG on the hepatic activities and mRNA expressions of the gluconeogenic enzymes phosphoenolpyruvate carboxykinase (PEPCK), fructose 1,6-bisphosphatase 1 (FBPase-1) and glucose 6-phosphatase (G6Pase). The activities are referred to the corresponding protein content (mg) and the mRNA expressions are given in arbitrary units (AU). Data are the mean  $\pm$  SEM of 4-7 animals. \* $p < 0.05$  and \*\* $p < 0.0001$ : different from Co; # $p < 0.05$  and ## $p < 0.0001$ : difference between MG100 and MG200.

both an anabolic energy-dependent conversion into glucose and a catabolic breakdown into lactate and pyruvate. Examination of the effects of MG on glycerol metabolism is, thus, an opportunity for evaluating how the compound affects both kinds of metabolism in a single experiment. Fig. 4A shows the time courses of glucose, lactate and pyruvate productions and oxygen consumption in perfused livers due to glycerol infusion. After the onset of glycerol infusion, the glucose and lactate productions were differently stimulated in the livers from controls and rats that received MG. The increment of glucose output due to glycerol (gluconeogenesis) is shown in Fig. 4B and it was approximately 40% lower in the liver from rats that received 100 and 200 mg/kg MG (compared to the controls). The glycerol infusion did not modify oxygen uptake in the liver of all groups, but the basal rate of oxygen uptake of the group that received 200 mg/kg MG was 20% lower than that observed in the controls and rats that received 100 mg/kg MG (Fig. 4C). The pyruvate production was a quite higher in the liver of rats that received 200 mg/kg MG, but there was not modified by glycerol. The lactate production was 63% and 285% increased by glycerol in the livers from the groups that received 100 and 200 mg/kg MG, respectively, when compared to the controls (Fig. 4D). Therefore, gluconeogenesis from glycerol was also impaired by MG, whereas oxidation to lactate plus pyruvate was increased by this compound.

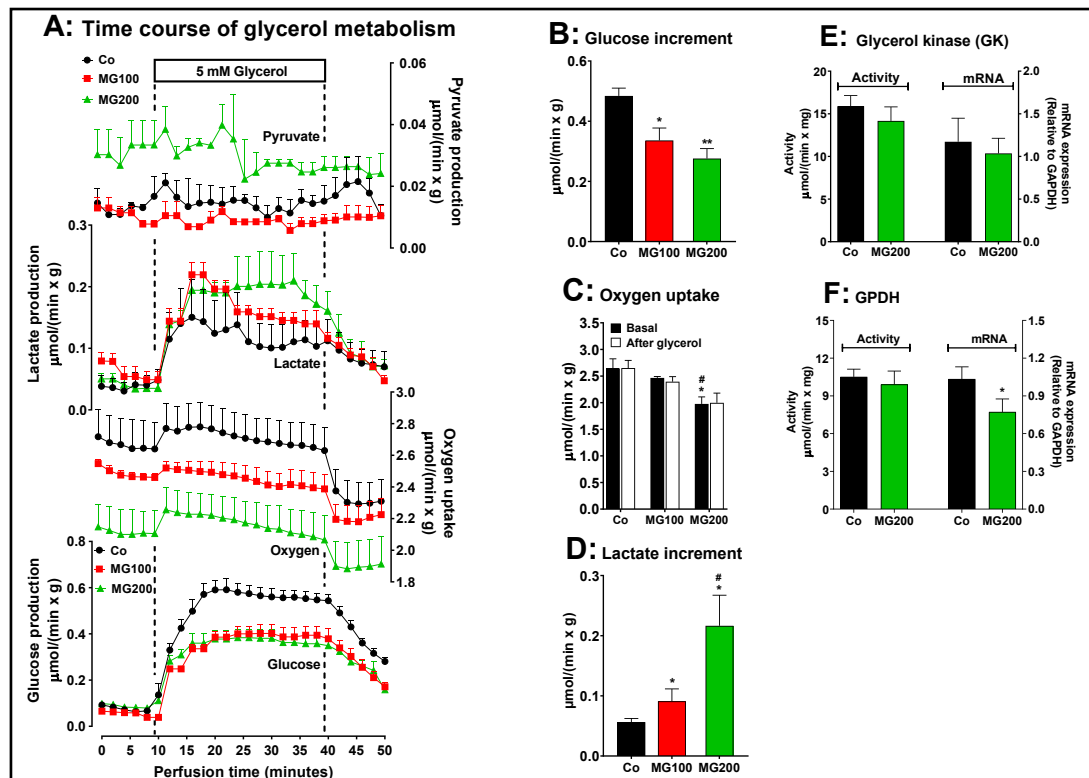


**Fig. 4.** Effects of MG on glycerol metabolism in perfused liver. Panel A: time courses of glucose, lactate and pyruvate production and oxygen consumption due to glycerol infusion. The animals received i.p. saline (Co), 100 or 200 mg/kg MG (MG100 and MG200) for 7 days. Livers from 12 h fasted rats were perfused with Krebs/Henseleit-bicarbonate buffer in combination with 5 mM D-glycerol as indicated by the horizontal box in Panel A. The outflowing perfusate was sampled in regular intervals and analyzed for its contents of glucose, lactate and pyruvate. Oxygen uptake was monitored by polarography. The values in Panels B and D are the increment of metabolites productions due to glycerol infusion. They were calculated from the data in Fig. 4A as [final values at the end of the infusion period with D-glycerol; 36 min] - [basal rates before infusion of D-glycerol; 8 min]. Panel C shows the oxygen consumption at the steady state in the basal period and after the infusion of glycerol. Panels E and F reveal the effects of MG on the hepatic activities and mRNA expressions of the specific enzymes involved in the gluconeogenesis from glycerol: glycerol kinase (GK) (panel E) and glycerol-3-phosphate dehydrogenase (GPDH) (panel F). The mRNA expressions are given in arbitrary units (AU). Data are the mean  $\pm$  SEM of 4-7 animals. \* $p < 0.05$  and \*\* $p < 0.0001$ : different from Co; # $p < 0.05$ : difference between MG100 and MG200.

The reactions catalyzed by glycerol kinase (GK) and glycerol-3-phosphate dehydrogenase (GPDH) are key steps for introducing glycerol into hepatic gluconeogenesis and glycolysis. Stimulation of these enzymes could be the cause of the increased lactate production from glycerol in the liver of rats receiving MG. Indeed, MG has been shown to increase GPDH activity in yeast [50]. Thus, the activity and mRNA expression of GK and GPDH were evaluated in rats receiving MG at 200 mg/kg and in control rats. The results are shown in Fig. 4E and 4F. These parameters were not significantly altered by MG, except for a slight reduction in GPDH mRNA expression, without affecting its activity. This indicates that a downstream event in these reactions may be stimulating glycerol oxidation and lactate accumulation in the liver of rats that received MG.

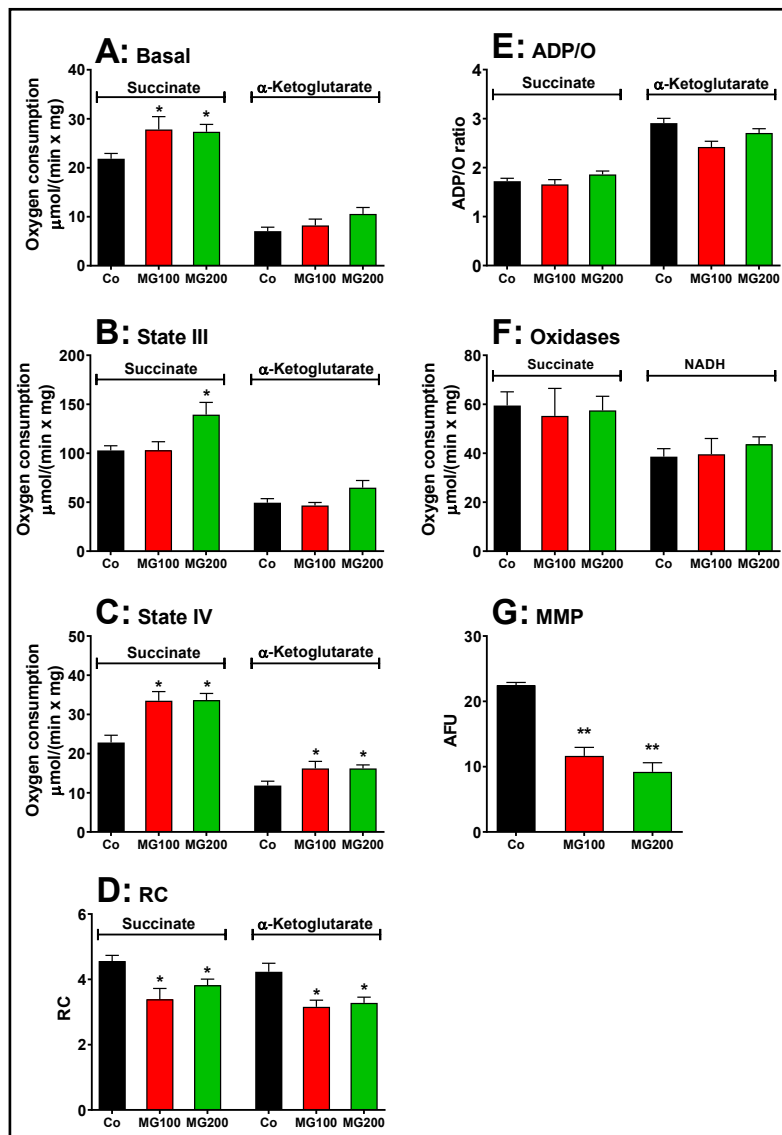
#### *MG modifies respiratory functions of isolated hepatic mitochondria*

The lactate accumulation caused by MG in the glycerol-perfused liver may be associated with the low efficiency of pyruvate transport into mitochondria within a short period. However, it may also result from mitochondrial alteration. In addition, MG not only reduced gluconeogenesis but also decreased hepatic oxygen consumption. Therefore, the respiratory activity and mitochondrial membrane potential (MMP) were evaluated in isolated liver mitochondria. The results are shown in Fig. 5. Basal respiration (before ADP addition), driven by succinate, but not by  $\alpha$ -ketoglutarate, was stimulated by approximately 25% in mitochondria of animals that received MG, when compared to the controls (Fig. 5A). State III respiration, also driven only by succinate, was stimulated by 35% in mitochondria of the group that received 200 mg/kg MG (Fig. 5B). State IV was stimulated in mitochondria of both groups that received MG by 47% and 37% when the respiration was driven, respectively, by succinate and  $\alpha$ -ketoglutarate (Fig. 5C). In consequence, the RC was reduced in mitochondria of both groups that received MG by 22% and 24% with succinate and  $\alpha$ -ketoglutarate, respectively (Fig. 5D). The ADP/O ratio, however, was not modified in animals which received both doses of MG (Fig. 5E). The activities of succinate and NADH oxidases were also not affected by the treatment with MG (Fig. 5F). The MMP was approximately 50% lower in mitochondria from animals that received MG when compared to the controls (Fig. 5E). Taken together, these results indicate that MG induces mild uncoupling and likely affects gluconeogenesis to a lesser extent than the inhibition of rate-limiting enzymes. Similarly, this phenomenon is unlikely to be the cause of lactate accumulation.

#### *MG decreases glycogen catabolism in the liver*

The production of lactate from glycerol was increased in perfused livers of rats which received MG. This indicates an increased flux of carbon units derived from this substrate through glycolysis. This raises the question if MG also modifies the flux of carbon units derived from endogenous glycogen. Livers from fed rats, when perfused with substrate-free medium, survive at the expense of glycogen degradation via glycolysis and oxidation of endogenous fatty acids [38, 51]. Under these conditions the liver releases glucose, lactate and pyruvate as a result of glycogen catabolism. Fig. 6A illustrates the time-courses of metabolic modifications in the perfused livers of the controls and rats that received MG. Four parameters were measured: glucose release, lactate and pyruvate productions and oxygen consumption. Most parameters presented fluctuations along the perfusion time. Glucose release, in particular, presented a tendency of declining. This tendency was strongest in the case of the livers from the group that received 200 mg/kg MG. The general tendency, however, was one of stabilization during the last 10 minutes of perfusion. For this reason, the data shown in panels B to G represent the mean values of each variable in the period between 25 and 30 min perfusion time. During this period of time, glucose release from livers of the group that received 200 mg/kg MG was approximately 50% lower than that one of livers from the controls (Fig. 6B). Glucose release from livers of the group that received 100 mg/kg MG was not different of that of livers from the controls. The same pattern was observed with lactate production (Fig. 6D), except that the decrease in the group that received 200 mg/kg MG reached 60%. The fluctuations in oxygen uptake (Fig. 6C) and pyruvate production (Fig.

**Fig. 5.** Effects of MG on respiratory activity and membrane potential of intact isolated hepatic mitochondria of rats. Hepatic mitochondria were isolated from animals which received i.p. saline (Co), 100 or 200 mg/kg MG (MG100 and MG200) for 7 days. For measuring the respiratory activity, intact mitochondria ( $1.0 \text{ mg} \cdot \text{mL}^{-1}$ ) were incubated at  $37^\circ \text{C}$  in a closed oxygraph chamber containing 2 mL reaction medium. The respiratory substrates were 10 mM succinate or  $\alpha$ -ketoglutarate. The respiration rates were measured under three conditions: (A) before the addition of ADP (basal respiration), (B) just after 0.125 mM ADP addition (state III respiration) and (C) after cessation of the ADP stimulation (state IV). The respiratory control (RC) was the ratio of state III/state IV (D) and the ADP/O ratio is defined as the number of moles of ADP phosphorylated per atom-gram of  $\text{O}_2$  consumption (E). The activities of succinate oxidase and NADH oxidase (F) were measured in freeze-thawing disrupted mitochondria using, respectively, succinate and NADH as substrates. The mitochondrial membrane potential (MMP) (G) was measured by spectrofluorimetry using the dye safranin and the results are expressed as arbitrary fluorescence units (AFU). Data are the mean  $\pm$  SEM of 4-7 animals. \* $p < 0.05$  and \*\* $p < 0.0001$ : different from Co.



6E) were not statistically significant. The changes in glycogenolysis and glycolysis, shown in panels F and G, show the same patterns as the changes in lactate production and glucose release. The lactate/pyruvate ratios, an indicative of the cytosolic NADH/NAD<sup>+</sup> ratio in the liver [20], were not different for all groups (results not shown). These results suggest that MG decreases glycogen storage, consistent with the catabolic state revealed by the previous experiments.

#### *MG modifies glucose and lipid homeostasis*

As MG altered adipose tissue weight and caused a substantial modification in hepatic carbohydrate metabolism, the next steps were to investigate whether this compound modifies systemic glucose and lipid homeostasis. Fig. 7 shows the results. Compared to the control group, fasting glycemia was 22% lower in the groups that received 100 and 200

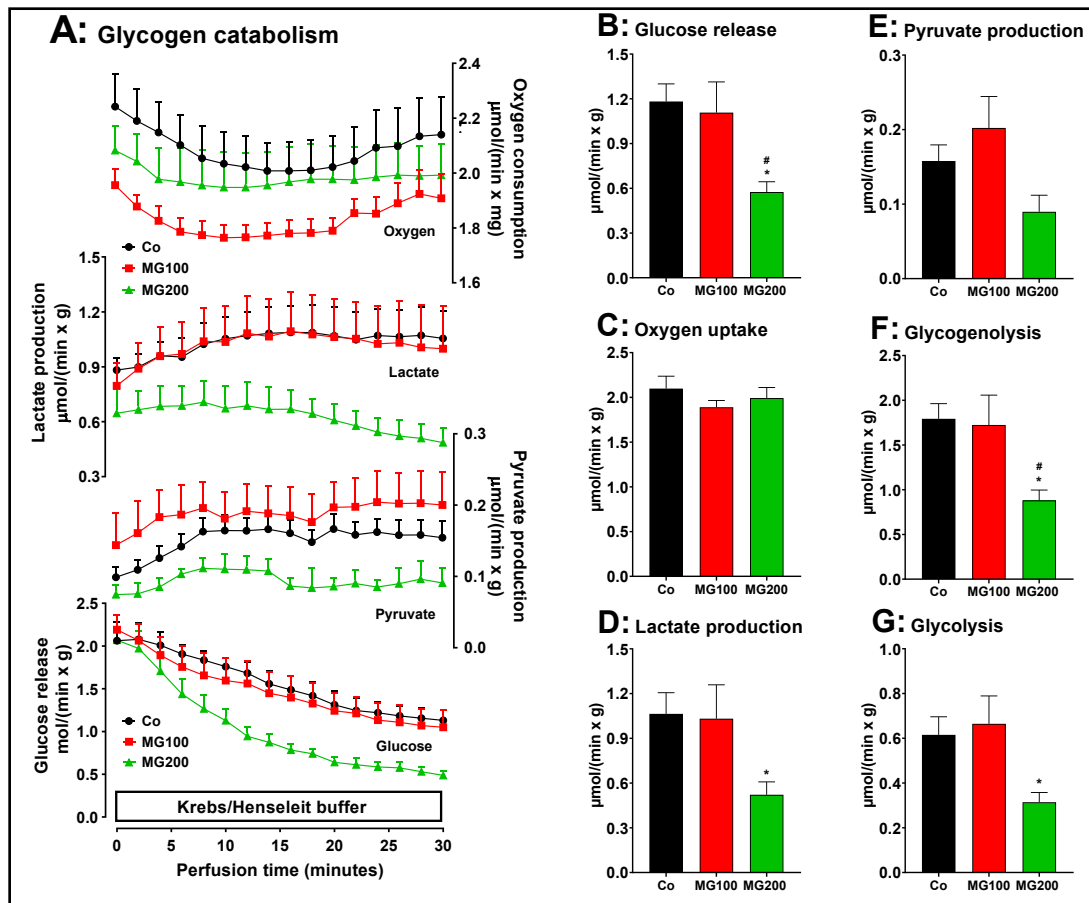


**Fig. 6.** Effects of MG on glycogen catabolism in perfused livers of fed rats. Panel A: time courses of glucose, lactate and pyruvate production and oxygen consumption. The animals received i.p. saline (Co), 100 or 200 mg/kg MG (MG100 and MG200) for 7 days. Livers from fed rats were perfused with substrate-free Krebs/Henseleit bicarbonate buffer. The outflowing perfusate was sampled in regular intervals and analyzed for its contents of glucose, lactate and pyruvate. Oxygen uptake was monitored by polarography. Data are the mean  $\pm$  SEM obtained from 5 animals for each condition. The values in Panels B, C, D and E are, respectively, the rates of glucose release, oxygen consumption, and lactate and pyruvate production observed after stabilization of the corresponding curves (26 min perfusion time). The values in Panels F and G were calculated from the rates of glucose, lactate and pyruvate production at 26 min perfusion time in Panel A. Glycogenolysis = glucose + 1/2(lactate + pyruvate) and glycolysis = 1/2(lactate + pyruvate). Each datum point represents the mean of 5 liver perfusion experiments. \* $p < 0.05$ : different from Co; # $p < 0.05$ : difference between MG100 and MG200.

mg/kg MG (Fig 7A; OGTT, time zero). The slopes of the initial increments in blood glucose were similar for all groups, but the initial level in the control condition (Co) was higher, the reason, possibly, why the peak value of the latter (30 min) was also higher. Return to the basal glycemia, however, occurred in the controls during the next 30 min, whereas no such return was observed for the animals that received MG. This may be indicating lower rates of glucose transformation. In the ITT (Fig. 7B), the response of the control was more pronounced, as indicated by the  $k_{ITT}$  values that were 40% lower in the groups that received 100 and 200 mg/kg MG (insert in Fig. 7B), although the starting points were different, suggesting that MG causes insulin resistance. Plasma and hepatic lipid profiles are shown in Figs. 7C and 7D. Compared to the controls, the levels of TAG were 28% lower in the plasma from rats that received 200 mg/kg MG (Fig. 7C). The total plasma cholesterol levels were not modified by MG, but HDL cholesterol was diminished. In the liver the content of total lipids

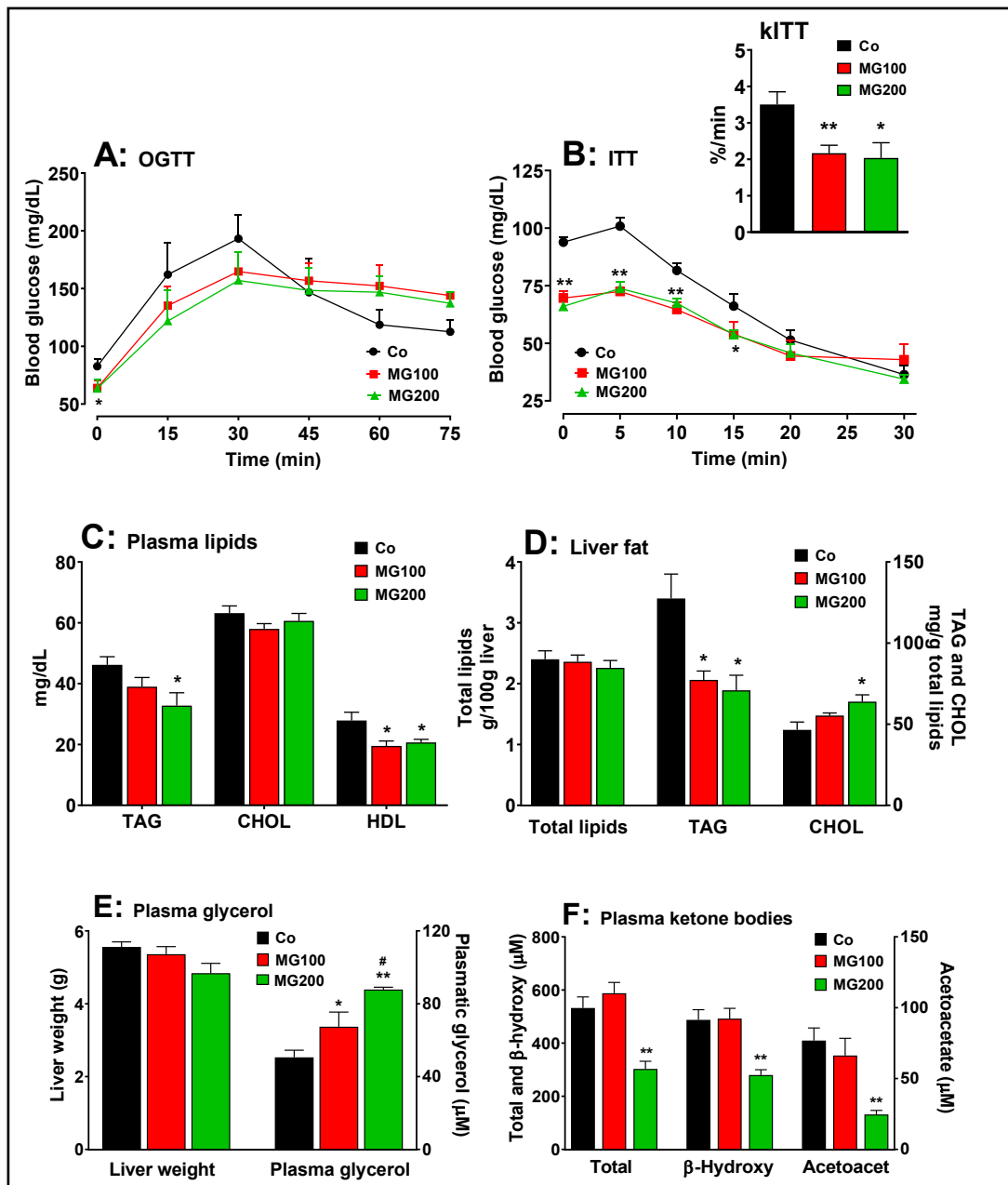


**Fig. 7.** Effects of MG on glucose and lipid homeostasis. A: fasting glycemia and oral glucose tolerance test (OGTT). B: insulin tolerance test and the rate constant for insulin tolerance test (kITT). C and D: Plasma and hepatic lipid profile, respectively. E: Liver weight and plasma glycerol. F: Plasma ketone bodies profile. The animals received i.p. saline (Co), 100 or 200 mg/kg MG (MG100 and MG200) for 7 days. OGTT was performed by oral administration of glucose (1.5 g/kg) to 12 h fasted rats. At indicated times, blood samples were taken from each animal by tail incision and glucose was measured using a glucometer. Fasting glycemia was measured immediately before glucose administration (at time zero in Panel A). ITT was performed by injecting regular insulin (1 U/kg body mass) i.p. into 12-h fasted rats with subsequent blood glucose measurement at the times indicated in panel B. kITT (inset in Panel B) was calculated as the slope of the linear segment of each curve (from time 5 to 20 in Panel C). The plasma levels of triglycerides (TAG), total cholesterol (CHOL), HDL cholesterol, glycerol, β-hydroxybutyrate (β-hydroxy) and acetoacetate (acetoacet) and the hepatic contents of total lipids, TAG and CHOL were assessed in 12 h fasted rats. Values are the mean ± SEM of 5-8 animals. \*p<0.05 and \*\*p<0.001: different from Co. #p<0.05: difference between MG100 and MG200.

was not affected by the MG treatment, but the TAG content was reduced by 35%, irrespective of the dose (Fig. 7D). The hepatic total cholesterol level, on the other hand, was 40% higher in the group that received 200 mg/kg MG. The liver weight was not modified by the MG treatment (Fig. 7E). The plasma levels of glycerol were 33% and 74% higher, respectively, in the groups that received 100 and 200 mg/kg MG, suggesting a higher lipolytic activity in the adipose tissue (Fig. 7E). The plasma levels of total ketone bodies,  $\beta$ -hydroxybutyrate and acetoacetate were, respectively, 44%, 43% and 68% lower in the group that received 200 mg/kg MG, but not modified in the group that received 100 mg/kg MG (Fig. 7F).

#### *MG increases hepatic ketogenesis from fatty acids*

The administration of MG modified lipolysis in adipose tissue and the levels of plasma ketone bodies. The latter are produced in the liver and measuring their production may be helpful in clarifying the action of MG. In the present study ketogenesis was measured in the perfused liver before and during palmitic acid infusion. Fig. 8A shows the time courses of  $\beta$ -hydroxybutyrate and acetoacetate productions and of oxygen uptake in perfused livers of fasted rats. There are differences in the basal rates among the various groups, but also differences in the stimulations caused by palmitate. To facilitate comparisons, Figs. 8B-I present, for all parameters, the basal rates (8 min perfusion time in Fig. 8A), the rates during palmitic acid infusion (28 min in Fig. 8A) and the absolute increments ( $\Delta$ ) caused by palmitic acid infusion (values at 28 min – values at 8 min). The onset of palmitic acid caused a stimulus in oxygen uptake ( $\sim 12\%$ ) in the livers of all groups (Figs. 8B and 8C). In the group that received 200 mg/kg MG the absolute increment in oxygen uptake was the highest (Fig. 8C). The basal rates of  $\beta$ -hydroxybutyrate production were not different among all groups and the onset of palmitic acid stimulated this parameter in the liver by  $\square 100\%$  in the controls and rats that received 100 mg/kg MG and 170% in the rats that received 200 mg/kg MG (Fig. 8D). Here again, the absolute increment was the highest in the in the group that received 200 mg/kg MG (Fig. 8E). The basal rates of acetoacetate production were 37% and 57% lower in the livers from rats which received 100 and 200 mg/kg MG (compared to controls), respectively, and palmitic acid increased all in similar proportions ( $\sim 30\%$ ) (Fig. 8F). Fig. 8G shows the  $\beta$ -hydroxybutyrate/acetoacetate ratios in the livers in the absence and presence of palmitic acid. The basal ratios were not statistically different in all groups before the infusion of palmitic acid, but upon infusion of the latter they were increased by 75% and 95% in the groups that received 100 and 200 mg/kg MG, respectively (Fig. 8G). No such increase was found when palmitic acid was infused in livers from the controls. Compared to the controls, the total ketone bodies production in the absence of palmitic acid was 37% and 43% lower in the livers from rats that received 100 and 200 mg/kg MG, respectively (Fig. 8H). Palmitic acid infusion increased the total ketone bodies production by 29%, 62% and 87%, respectively, in the controls, group that received 100 mg/kg MG and group that received 200 mg/kg MG (Fig. 8H). In absolute terms, the increment in total ketone bodies production caused by palmitic acid was highest in livers of rats that received 200 mg/kg MG (Fig. 8I).

#### *MG modifies the AMPK levels and activation in the adipose tissues*

The AMP-activated protein kinase (AMPK) plays a major role in the regulation of hepatic and adipose tissue metabolism [52]. Therefore, the protein levels of AMPK and phosphorylated (activated) AMPK (p-AMPK) were determined in the liver and adipose tissues. A representative western blot quantifying the relative levels of AMPK, p-AMPK, and actin in the samples is shown in Fig. 9A, with the sample for a single condition loaded into each lane (vertical column). The results of densitometric analysis of the respective western blots for AMPK and the p-AMPK/AMPK ratio are shown in Fig. 9B-G. The p-AMPK/AMPK ratio represents the AMPK activity. MG at both doses did modify neither the level of AMPK nor the ratio p-AMPK/AMPK in the liver (Fig. 9B and C). MG at both doses reduced by 70% the AMPK levels in mesenteric fat, but the ratio p-AMPK/AMPK was not modified in this tissue (Fig. 9D and E). In the retroperitoneal adipose tissue, MG at both doses increased by 58% the AMPK levels, but the ratio p-AMPK/AMPK was increased only in the group that received 200 mg/kg MG (180%; Fig. 9F and G).

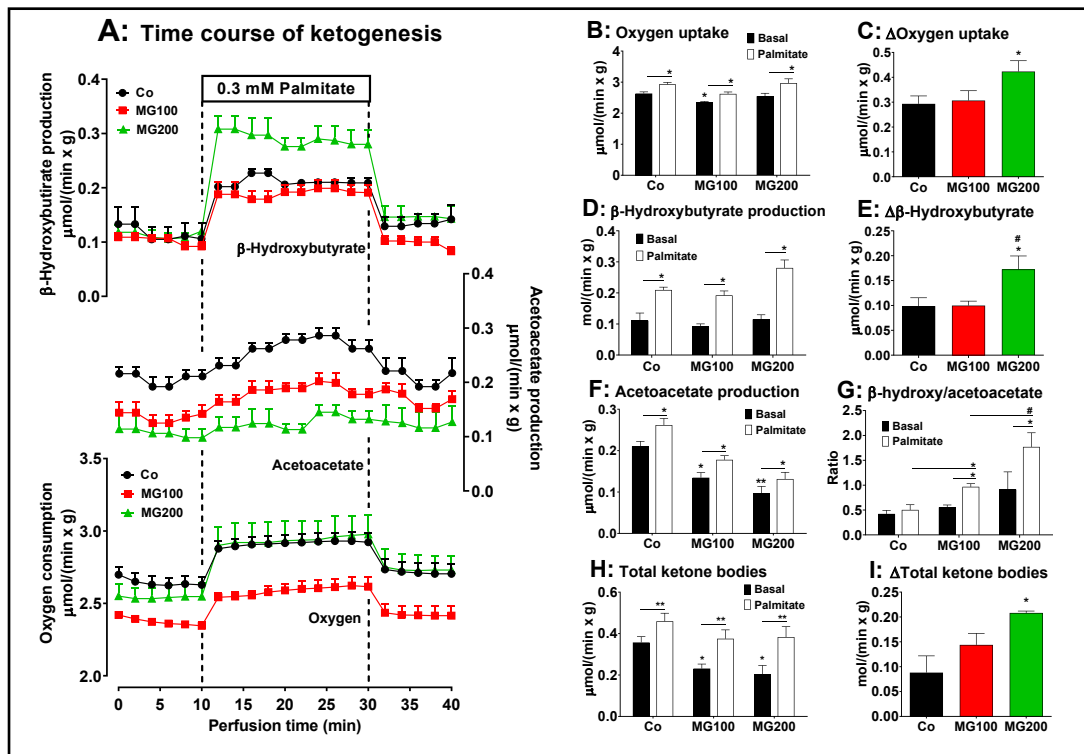


**Fig. 8.** Effects of MG on ketone bodies production from palmitic acid in the liver. Panel A: time courses of  $\beta$ -hydroxybutyrate and acetoacetate productions, and oxygen consumption due to palmitic acid infusion. The animals received i.p. saline (Co), 100 or 200 mg/kg MG (MG100 and MG200) for 7 days. Livers from 12 h fasted rats were perfused with Krebs/Henseleit bicarbonate buffer in combination with 0.3 mM palmitic acid as indicated by the horizontal box in Panel A. The outflowing perfusate was sampled in regular intervals and analyzed for their contents of  $\beta$ -hydroxybutyrate and acetoacetate. Oxygen uptake was monitored by polarography. Panels B, D, F and H show the values of the liver metabolites output at the basal steady-states (8 min in Panel A; black bars) and the steady-states after palmitic acid infusion (28 min in Panel B; white bars). Panel G shows the values of the  $\beta$ -hydroxybutyrate/acetoacetate ratio in the liver at the basal steady-state and at the steady-state after palmitic acid infusion. The values in Panels C, E and I are the increments of the metabolites productions due to palmitic acid infusion and were calculated from the data in Fig. 8A as [final values at the end of the infusion period with palmitic acid; 28 min] - [basal rates before infusion of palmitic acid; 8 min]. Each datum point represents the mean of 4-5 liver perfusion experiments. \* $p < 0.05$  and \*\* $p < 0.001$ : different from Co. # $p < 0.05$ : difference between MG100 and MG200.

### MG causes hepatic inflammation

The effects of MG on the systemic inflammation and liver damage were investigated because MG is associated with liver inflammation even in the absence of steatosis [53]. The ALT and AST activities were assayed in the plasma to evaluate liver damage. The results are shown in Fig. 10A and B. The AST activity was only slightly increased in the plasma in both groups that received MG (~60%), but no changes were found in the ALT activity. The latter is regarded as a specific marker of hepatic damage, but AST may be increased in diseases of other organs such as muscle and heart [54]. AST elevations under 100% are normally regarded discrete and not evidence of significant liver damage [54, 55]. The levels of total proteins and albumin, and MPO activity in the plasma were assayed as markers of systemic inflammation. The MPO activity was approximately 60% higher in the plasma of animals that received MG (Fig. 10C). Total protein was reduced only in the plasma from rats that received 200 mg/kg MG (15%), but albumin levels were reduced by 12% and 22% respectively in rats that received 100 and 200 mg/kg MG (Fig. 10D and E). As consequence, the albumin/

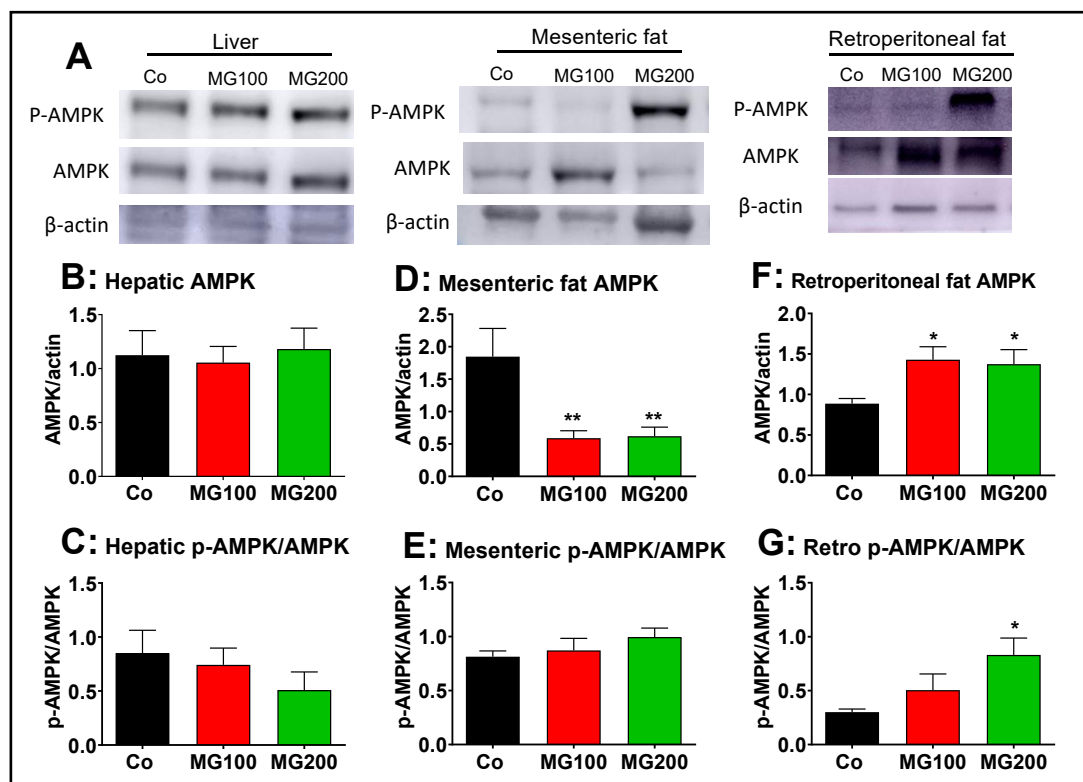


**Fig. 9.** Western blot analysis of the AMP-activated protein kinase (AMPK) and the phosphorylated (activated) form of AMPK (p-AMPK) in liver and fat tissues. Analyses were performed with the hepatic and fat tissues of 12 h fasted rats which received i.p. saline (Co), 100 or 200 mg/kg MG (MG100 and MG200) for 7 days. A: Representative western blot quantifying the relative levels of AMPK, p-AMPK, and actin, with the sample for each single condition loaded onto each lane (vertical column). The results of densitometric analysis of the respective western blots are presented in Panels B for hepatic AMPK, D for mesenteric fat AMPK and F for retroperitoneal fat AMPK. C, E and G show the p-AMPK/AMPK ratios, respectively, for hepatic, mesenteric fat and retroperitoneal fat tissues. Values are the mean  $\pm$  SEM of 6 animals. \* $p < 0.05$  and \*\* $p < 0.001$ : different from Co.

globulin ratio was reduced by approximately 50% in the plasma of both groups (MG100 and MG200; Fig. 10F). The hepatic MPO activity, an indicative of polymorphonuclear leukocytes infiltration in the organ, was 100% higher in rats which received MG (Fig. 10G). The expressions in terms of mRNA of the interleukin (IL) 1 $\beta$ , IL-6, tumoral necrosis factor alpha (TNF $\alpha$ ) and sirtuin 1 (SIRT1) were determined in the hepatic tissue of controls and animals that received 200 mg/kg MG. The results are shown in Fig. 10H-10J. The expression of IL-1 $\beta$  and TNF $\alpha$  was not modified, but the expression of IL-6 mRNA was 5-fold higher in livers from rats that received MG (compared to the controls). The expression of SIRT1 was downregulated by MG. SIRT1 is an NAD<sup>+</sup>-dependent deacetylase enzyme that inhibits NF- $\kappa$ B and, at the same time, has its expression suppressed by IL-6. Taken together, these results show that MG causes hepatic and systemic inflammation.

#### *MG promotes systemic and hepatic oxidative stress*

The effects of MG on oxidative stress were assessed in the plasma and liver. The reason is that inflammation is normally associated with an increase of oxidative stress in different organs [55-58]. The levels of protein carbonyl groups, a marker of oxidative injury to proteins, were 45% higher in the plasma of both groups that received MG (compared to the control; Fig. 11A). The levels of thiol groups, an antioxidant marker, were 32% and 48% lower in the plasma from rats that received 100 and 200 mg/kg MG, respectively (Fig. 11B). TAC was

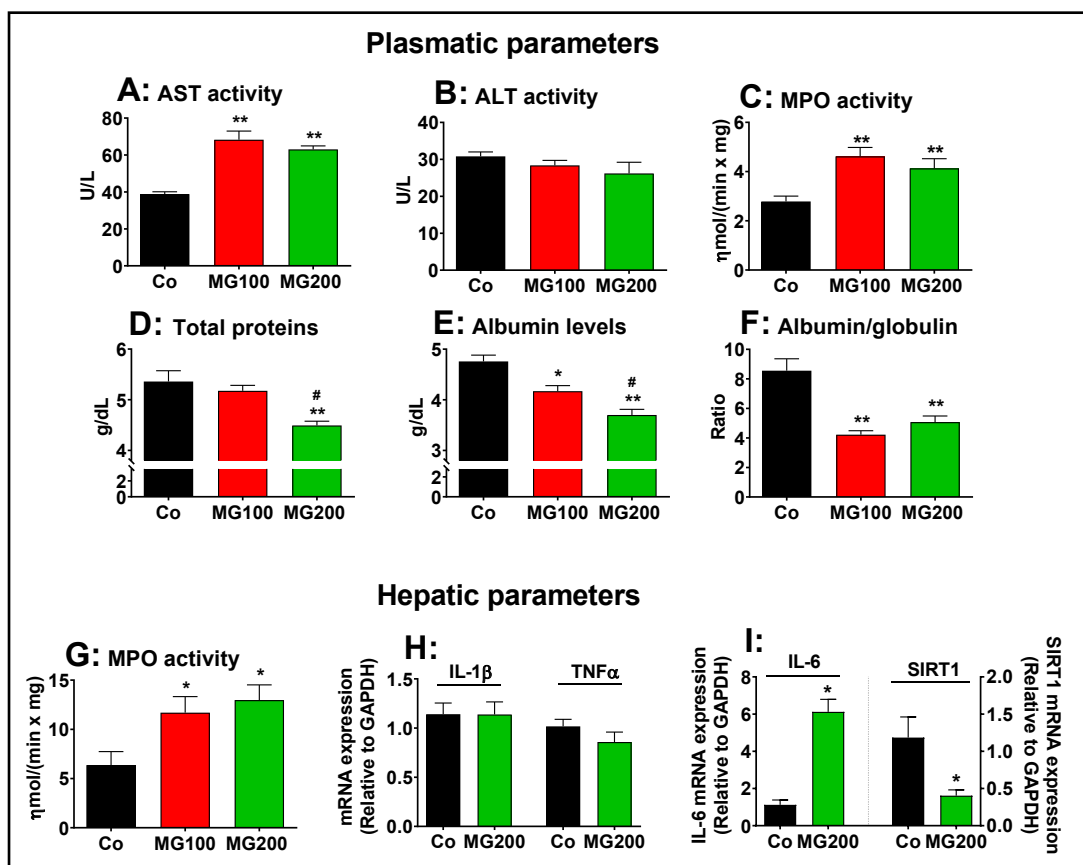


**Fig. 10.** Markers of systemic and hepatic damage and inflammation. The parameters were determined in plasma and liver of 12 h fasted rats which received i.p. saline (Co), 100 or 200 mg/kg MG (MG100 and MG200) for 7 days. The mRNA expressions of IL-1 $\beta$ , IL-6, TNF $\alpha$  and SIRT1 were determined in the hepatic tissue by qRT-PCR. The activity of myeloperoxidase (MPO) was assayed in plasma and hepatic tissue. The activities of aspartate aminotransferase (AST), alanine aminotransferase (ALT) and the levels of total proteins and albumin were assayed in plasma. The level of globulin was calculated by subtracting albumin from total proteins. Data represent the mean  $\pm$  SEM of 6 animals. \* $p$ <0.05 and \*\* $p$ <0.001: different from Co.

68% lower in the plasma from rats that received MG, but FRAP was lower (30%) only in the group that received 200 mg/kg MG (Fig.11C). Figs. 11D-N show the oxidative status of the liver. The levels of protein carbonyl groups were 47% and 160% higher, respectively, in the livers from rats that received 100 and 200 mg/kg MG (Fig. 11D). The levels of ROS were 47% higher in the liver of both groups that received MG (Fig. 11E). The catalase activity was 20% and 40% lower, respectively, in the livers from rats that received 100 and 200 mg/kg MG (Fig. 11F). The SOD activity was lower (20%) only in the liver from rats that received 200 mg/kg MG (Fig. 11F). Since catalase activity was more strongly inhibited, its mRNA expression was measured in the liver of rats treated with 200 mg/kg MG and was found to be reduced by 80% (Fig. 11J). The hepatic levels of GSH were not different among all groups, but the levels of GSSG were 25% higher in the group that received the highest dose of MG (Fig. 11G and H). In consequence, the GSH/GSSG ratio was 36% lower in the livers of this group (Fig. 11I), indicating an impairment in GSH regeneration. The GSH/GSSG ratio is affected by the balance between enzymes involved in GSH consumption and generation. In order to explain this finding, the expression in terms of mRNA of GPx1, GR, HO-1 and GSTA3 was determined in the hepatic tissue of controls and animals that received 200 mg/kg MG. The results are shown in Fig. 11K-N. The expressions of GR and GPx1 were not modified, but GSTA3 expression in the liver was 50% lower in rats that received 200 mg/kg MG compared to the controls. Notably, 200 mg/kg MG increased hepatic HO-1 expression by 75%. The total glutathione, however, was not modified by MG (results not shown). These results show that MG increases systemic and hepatic oxidative stress.

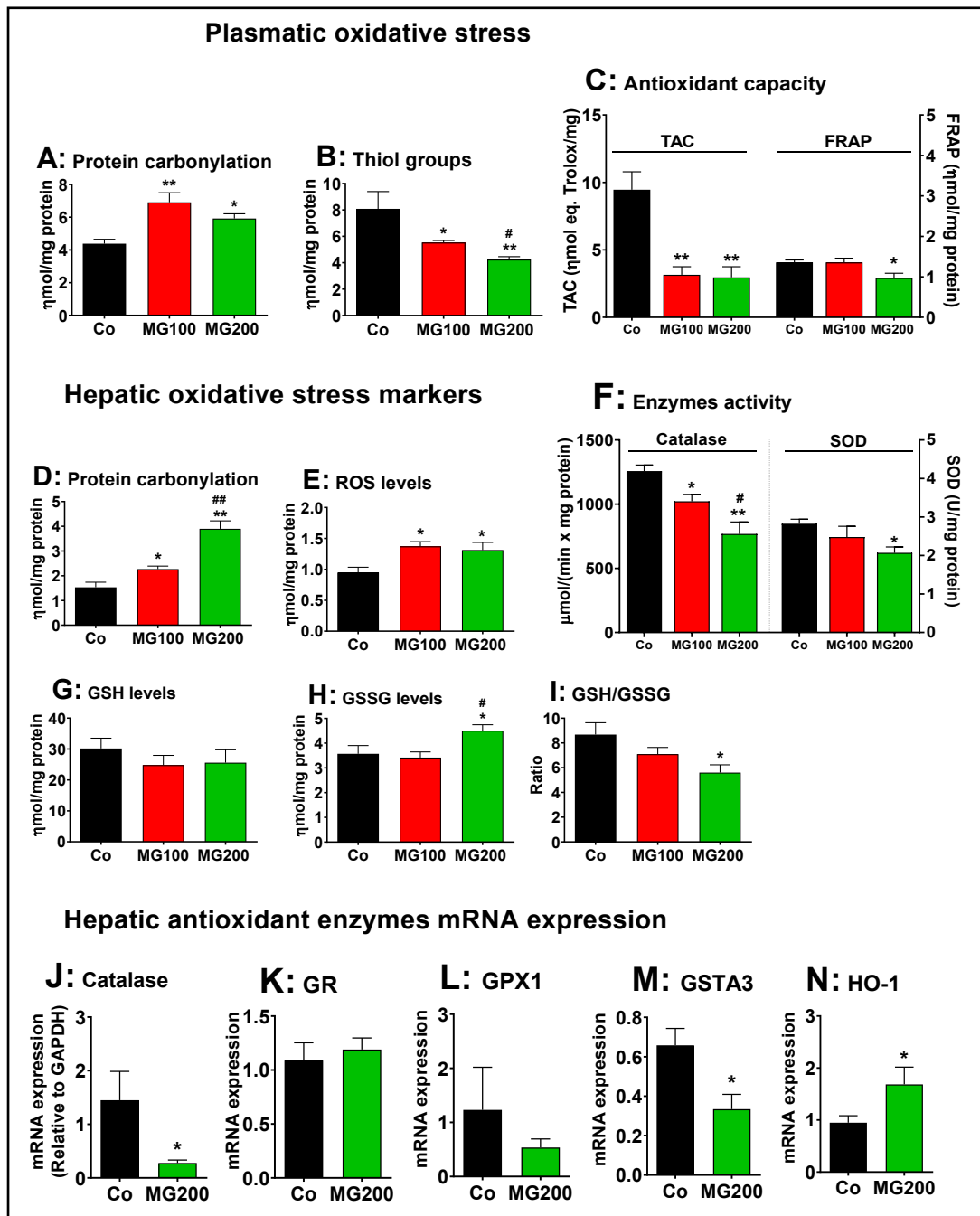


**Fig. 11.** Effects of MG on the oxidative status of plasma and liver. The parameters were determined in the plasma and liver of 12 h fasted rats which received i.p. saline (Co), 100 or 200 mg/kg MG (MG100 and MG200) for 7 days. Panels A – C present markers of plasmatic oxidative stress, respectively protein carbonylation (A), thiol groups (B), TAC (total antioxidant activity of plasma) and FRAP (ferric reduction capacity of plasma) (C). Panels D – I show markers of hepatic oxidative stress, respectively protein carbonylation (D), ROS content (E), catalase and SOD activity (F), GSH (reduced glutathione) content (G), GSSG (oxidized glutathione) content (H) and GSH/GSSG ratio (I). The mRNA expressions (normalized to GAPDH) of hepatic antioxidant enzymes are shown in panels J (Cat: catalase), K (GR: glutathione reductase), L (GPx1: glutathione peroxidase 1), M (GSTA3: glutathione-S-transferase) and N (heme oxygenase 1, HO-1). Data represent the mean  $\pm$  SEM of 5-8 animals. \* $p < 0.05$  and \*\* $p < 0.001$ : different from Co. # $p < 0.05$  and ## $p < 0.001$ : difference between MG100 and MG200.

*MG increases the AGE content and upregulates RAGE expression in the liver*

The levels of MG and AGE were quantified in the plasma and liver of rats to measure the extent to which these compounds increased in these tissues. The peak of MG concentration in plasma is reported to be reached at 4 h after a single oral dose, returning to baseline levels 8 h after, regardless of whether 100 or 200 mg/kg was administered [25]. A high MG level in the plasma of rats is sustained after 3 consecutive days of administering a 100 mg/kg dose [25]. Then, the levels of MG were assayed in the plasma of rats 4 h and 12 h after the administration of the 200 mg/kg dose on the seventh day (the last day of MG administration).

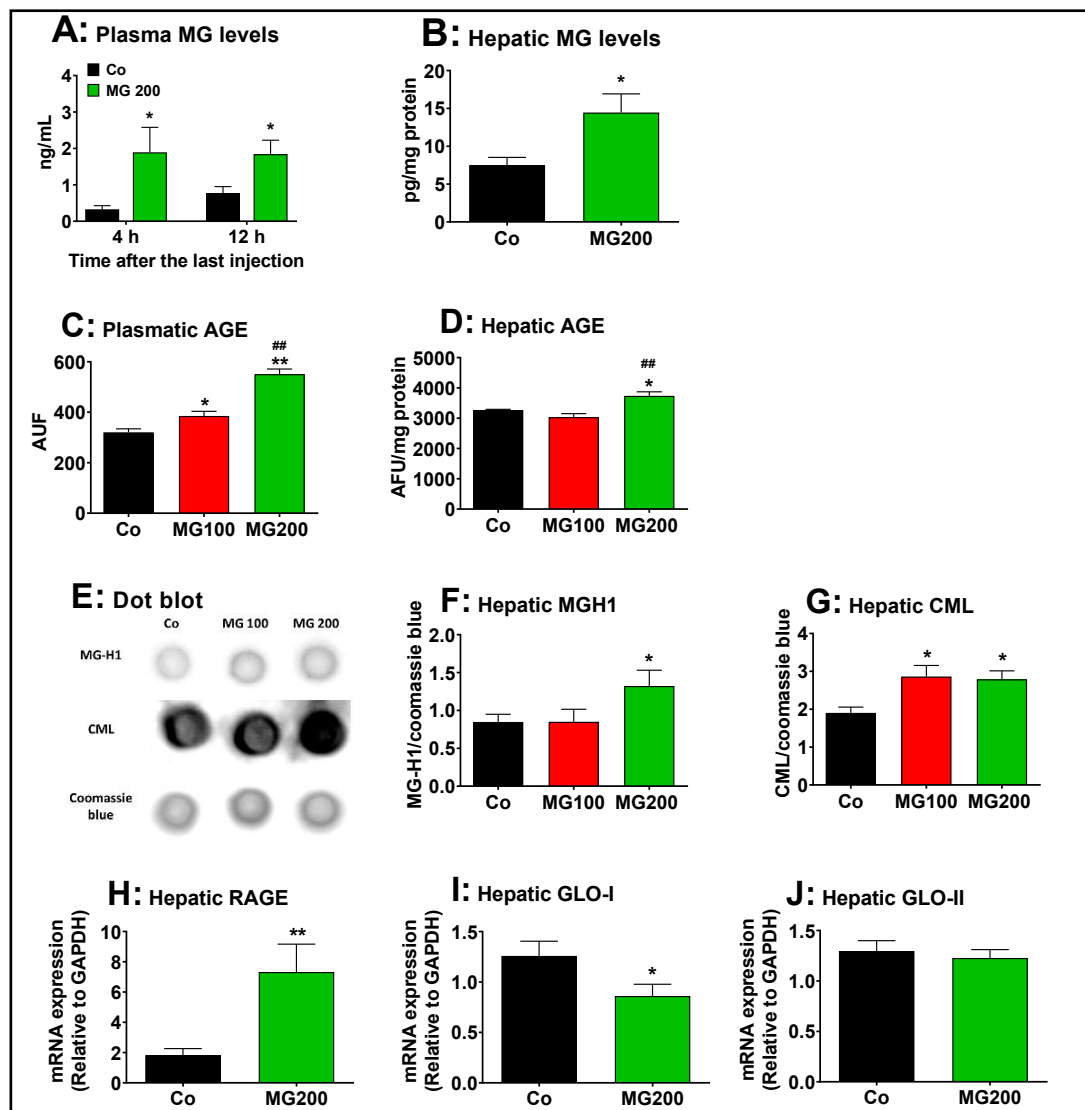


**Fig. 12.** Effects of MG on AGE content, RAGE expression and glyoxalases activity in the liver. A and B: levels of MG in plasma and liver, respectively. Plasmatic MG was assayed after 4 and 12h after the last injection of MG in fasted rats. The remaining analyses were performed in liver and plasma 12h after the last injection of MG in fasted rats, which received i.p. saline (Co), 100 or 200 mg/kg MG (MG100 and MG200), for 7 days. C and D: the levels of AGE in plasma and liver, respectively. E: representative dot blot quantifying the relative levels of carboxymethyllysine (CML), methylglyoxal-hydroimidazolone 1 (MG-H1) and coomassie blue, with the sample for each single condition loaded onto each lane (vertical column). The results of densitometric analysis of the respective dot blot are presented in Panels F for MG-H1 and G for CML. H: the RAGE mRNA expression in the liver. I and J: expression of glyoxalase I (GLO-I) and glyoxalase II (GLO-II) in the liver, respectively. Values are the mean  $\pm$  SEM of 4-8 animals. \* $p < 0.05$  and \*\* $p < 0.001$ : different from Co. ## $p < 0.001$ : difference between MG100 and MG200.

The results are shown in Fig. 12A. The control rats showed MG levels ranging between 0.4 and 0.7 ng/mL. MG administration raised their plasma levels to approximately 2 ng/mL at both 4 and 12 hours post-dosing. The levels of MG were 70% higher in the liver of rats 12 h after the administration of the 200 mg/kg dose on the seventh day (Fig. 12B).

The content of AGE generated by the reaction of MG with proteins was determined in the plasma and liver. The results are shown in Figs. 12C and 12D. The plasma levels of AGE were 20% and 72% higher respectively in the groups that received 100 and 200 mg/kg MG, respectively (Fig. 12C). In the liver, the levels of AGE were higher (14%) only in the rats that received 200 mg/kg MG (Fig. 12D). Next, the contents of CML and MG-H1 were assayed in the liver. These compounds are the main AGE associated with proteins generated by reaction with MG [3]. A representative dot blot quantifying the relative levels of MG-H1 and CML in liver samples is shown in Fig. 12E, with the samples for each condition displayed vertically. The results of the densitometric analysis of the respective dot blots for MG-H1 and CML are presented in Figs. 12F and 12G, respectively. The levels of MG-H1 were 55% higher in the liver from rats that received 200 mg/kg MG, but the levels of CML were approximately 50% higher in the livers of both groups that received MG. The expressions of RAGE, GLO-I and GLO-II in terms of mRNA were assayed only in the livers from rats which received 200 mg/kg MG. The results are shown in Fig. 12H-J. The expression of RAGE was three-fold higher in the liver from rats that received 200 mg/kg MG (compared to Co). The expression of GLO-I was 32% lower in the livers from rats that received MG, but the expression of GLO-II was not modified. These results reveal that MG administration increases AGE production in plasma and liver while upregulating hepatic RAGE expression, a phenomenon associated with increased inflammation and oxidative stress.

#### *MG and AGE increase human lymphocyte viability*

The content of MG and AGE was increased in plasma and MG upregulated inflammatory pathways in the liver and systemically. Lymphocytes are directly associated with the immune response to inflammation and they make up around 40% of the circulating white blood cells in humans. This leads to the hypothesis that both MG and MG-derived AGE may stimulate the proliferation of these cells and modify their viability. Human lymphocytes were used to test this hypothesis. The characterization of the AGE was performed to verify whether its preparation was adequate. The AGE preparations were characterized in relation to non-oxidized amino acids, Maillard compounds, protein carbonyl groups, protein sulfhydryl groups, N-oxidation of protein amino acids, and contents of CML and MG-H1. The results are presented as Supplementary Materials (Fig. S1) and show that the method used was effective in producing AGE.

The cells were cultured in the presence of MG or AGE by 24 or 48 h, and their viability was evaluated by the MTT method. The results are shown in Fig. 13. Incubation for 24 h with MG up to 100  $\mu$ M and MMS (positive control) reduced only slightly viability (10% to 20%). However, more pronounced reductions were found with MG at the concentrations of 500  $\mu$ M (30%) and 1000-2000  $\mu$ M (> 80%; Fig. 13A). When the incubation time was increased to 48 h, the viability of the lymphocytes was reduced by approximately 70% with 1000 and 2000  $\mu$ M MG and MMS. Lower concentrations of MG (5–500  $\mu$ M), however, increased viability by approximately 40% (Fig. 13B). For investigating lymphocyte viability in the presence of AGE, the latter were produced as described in section 2.17. Lymphocytes viability was evaluated with BSA (negative AGE), AGE-L and AGE-H at the concentrations of 0.1, 1.0 and 2.5 mg/mL, respectively, during 24 and 48 h. The results are shown in Figs. 13C and 13D. Incubation of lymphocytes for 24 h with BSA increased viability by approximately 45%, but incubation with AGE-L and AGE-H caused increases of 100% and 120%, respectively (Fig. 13C). BSA treatment did not increase lymphocyte viability when the incubation was extended further to 48 h, but the AGE-L and AGE-H treatment still promoted 20 to 30% increases, respectively, during this extended time period (Fig. 13D).

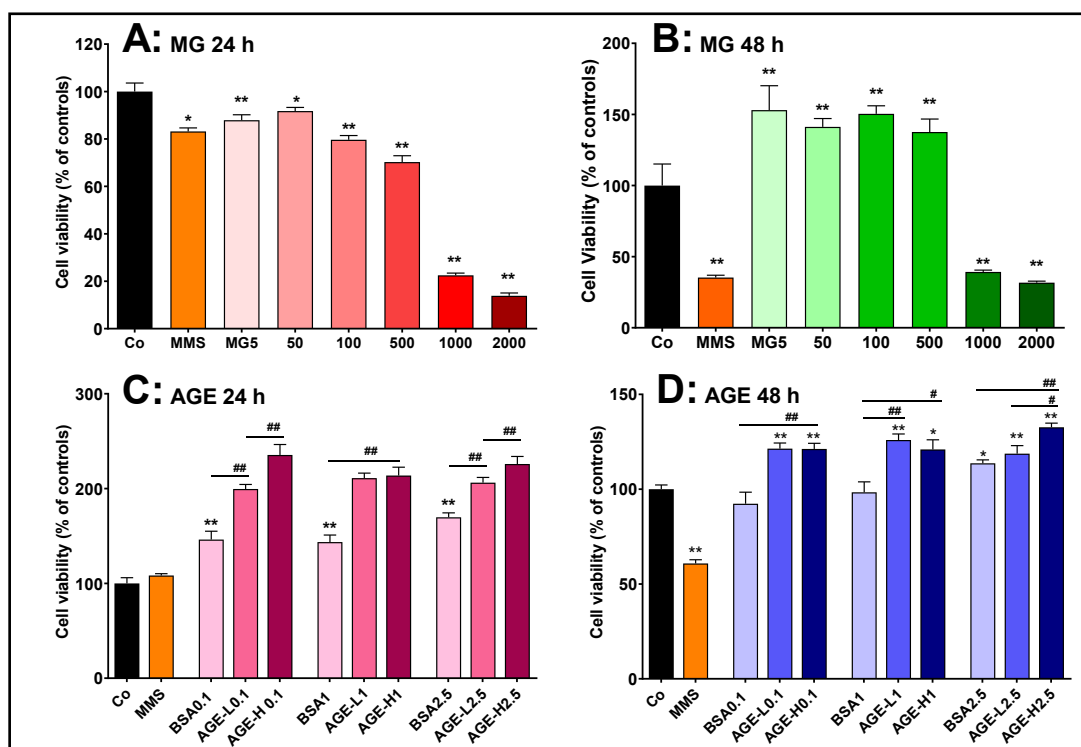


**Fig. 13.** Effects of MG and AGE on cell viability of human peripheral lymphocytes in vitro. AGEs were produced by incubating bovine serum albumin (BSA) with 50 mM (AGE-L) or 250 mM (AGE-H) MG. Lymphocytes were obtained from human peripheral blood from four healthy male donors and cells were cultured at 37 °C in 96-well plates containing RPMI medium supplemented with FBS. The lymphocytes viability was evaluated by the MTT method. A and B: cell viability of lymphocytes that were incubated with MG at concentrations in the range of 5-2000 µM during 24 h and 48 h, respectively. C and D: cell viability of lymphocytes that were incubated with AGE at concentrations of 0.1, 1 and 2.5 mg/mL during 24 h and 48 h, respectively. MMS (methyl methanesulfonate) was employed as positive control. Values are the mean ± SEM of 4 experiments. \* $p < 0.01$  and \*\* $p < 0.001$ : different from Co. # $p < 0.01$  and ## $p < 0.001$ : difference indicated by the supper lines (—).

## Discussion

### General aspects

In general terms it is apparent from the results of the present work that MG administered to healthy rats causes systemic inflammation and metabolic changes similar to diseases associated with a widespread catabolism in the body: reduction of food intake, loss of lean mass, increase of lipolysis and lower body weight gain. MG also influences the metabolism in adipose tissues and liver in several ways. The most important events are illustrated by Fig. 14, which utilizes the data of this work to represent in a schematic way the integrated metabolic modifications occurring in adipose tissues and liver of rats that received MG. These events will be discussed in the following paragraphs.

### Inflammation and oxidative status

The administration of MG for seven days increased its levels in the plasma for 2-4 times and in the liver by approximately 2 times, similar to those observed in patients with cirrhosis and diabetes, and rats with  $\text{CCl}_4$ -induced hepatitis [17, 59, 60]. These high levels of MG increased the hepatic and serum levels of AGE and caused systemic inflammation in healthy rats. CML and MG-H1 are the main adducts (AGE) formed by the reaction of MG with proteins and they were increased in the liver. This shows that proteins, including enzymes, are being

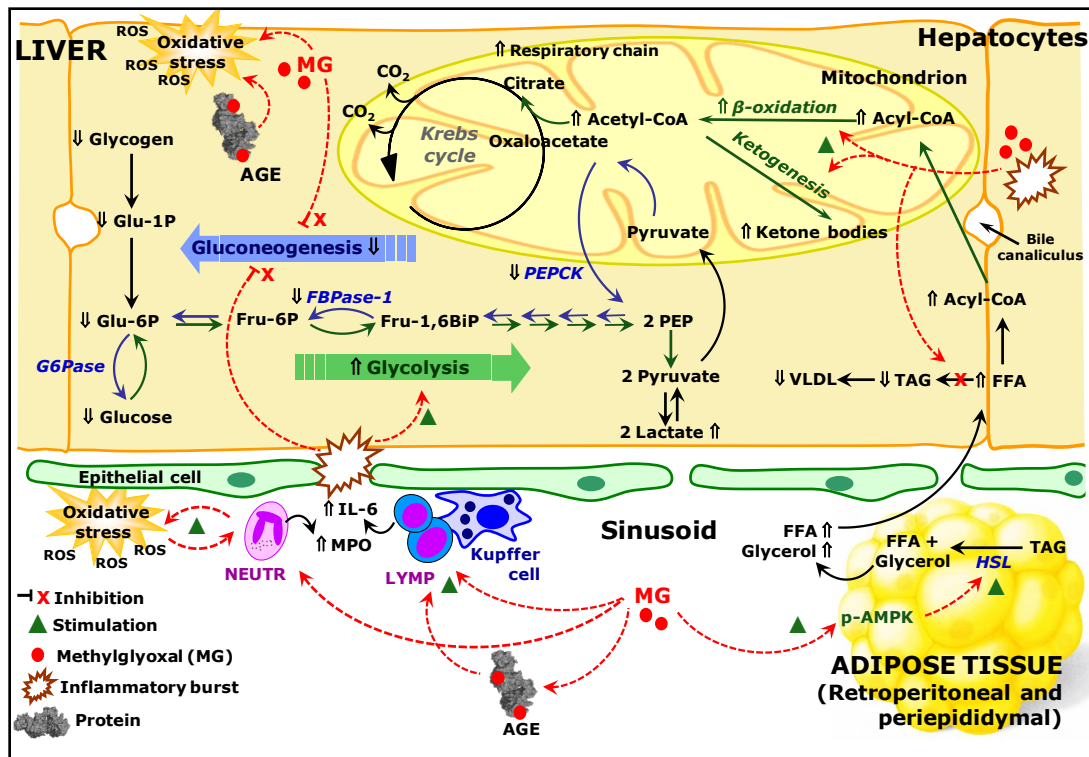


**Fig. 14.** Schematic representation of the effects of MG on inflammation and metabolic pathways in the liver and adipose tissue of rats. The scheme is discussed in the text and is based on the results of the current work. The symbol  $\uparrow$  means up-regulation and  $\downarrow$  down-regulation. Red arrows indicate effects of methylglyoxal (MG). Abbreviations: MPO, myeloperoxidase; IL-6, interleukin 6; FFA, free fat acids; TAG, triglycerides; VLDL, very low density lipoprotein; HSL, hormone sensible lipase; AGE, advanced glycation end products; PEP, phosphoenolpyruvate; Glu-6-P, glucose 6-phosphate; Fru-6-P, fructose 6-phosphate; Fru-1,6-BiP, fructose 1,6-bisphosphate; G6Pase, glucose 6-phosphatase; PEPCK, phosphoenolpyruvate carboxykinase; FBPase-1, phosphofructokinase 1; CoA, coenzyme A; ROS, reactive oxygen species; LYMP, lymphocytes, NEUTR, neutrophils.

structurally modified by MG and, by consequence, they can be functionally impaired. The reduced GLO-I mRNA expression must be contributing to elevate even more the levels of AGE in the liver. In fact, the higher production of MG in diabetes and obesity has been related with the downregulation of GLO-I [3, 61].

Increases in MPO activity in the plasma and liver correspond, respectively, to leukocytosis and infiltration of inflammatory cells in the organ, which was followed by increases of IL-6 expression. Together, inflammation and AGE are likely to be acting synergistically to upregulate the RAGE expression, which should increase even more liver inflammation. In the present study, both MG and AGE were able to increase lymphocyte viability *in vitro*. This agrees with observations that MG promotes macrophage activation and lymphocyte proliferation, and that AGE-RAGE interaction induces lymphocyte proliferation [62, 63]. Furthermore, the activation of inflammatory cells by MG leads to the production of cytokines, particularly IL-6, which induces NF- $\kappa$ B activation, RAGE expression and severe cirrhosis [17]. In addition, the reduced expression of SIRT1 in the liver of rats that received MG can further exacerbate these effects, as this enzyme inhibits NF- $\kappa$ B and decreases hepatic fibrosis [64].

Advanced liver diseases, such as cirrhosis, are normally associated with liver damage. However, not always systemic inflammation is accompanied by liver injury [55]. Plasma markers of liver damage were only slightly increased in rats that received MG, more specifically, only the AST activity was somewhat increased, a finding that indicates moderate liver damage [54, 55]. However, this phenomenon is the same occurring in patients with

advanced cirrhosis, in which only a moderate elevation of AST activity is associated with impaired liver function, reduced albumin levels and high levels of circulating MG and IL-6 [17]. The levels of albumin and the ratio of albumin/globulin were reduced in the liver of rats that received MG, however, both systemic inflammation and liver damage are associated with these changes. It is therefore possible that MG causes a high-grade systemic inflammation with mild liver damage.

MG led to increases in the levels of ROS and protein carbonyl groups, a pro-oxidative marker, in the liver. The plasma levels of protein carbonyl groups were also increased and the antioxidant capacity was reduced. This increased oxidative stress is probably the result of both systemic inflammation and direct action of MG on proteins. In fact, carbonylation of proteins occurs by the reaction with ROS and also when MG reacts with amino and sulfhydryl groups [3, 32] (Fig. S1 in Supplementary Materials). It is worth to emphasize that the sulfhydryl groups (thiols) of albumin account for 70% of the antioxidant capacity of the plasma [32]. In the liver, GSH is an intracellular antioxidant and it is also used to detoxify MG in the reaction of GLO-I and II. The hepatic GLO-I expression was reduced, and GSH levels were unaffected. However, the GSH/GSSG ratio was decreased in the liver due to an increase in GSSG levels, which is indicative of oxidative stress. The GSSG accounts for less than 10% of the total glutathione (GSH plus GSSG) in the healthy liver [55], but it seems, at least in part, that there is an impairment in GSH regeneration. The expression of GR and GPx1 was not altered, indicating that this impairment may be due to either a reduction in the activity of these enzymes caused by direct action of MG or a limitation in the availability of the electron donor NADPH. Anyway, GSH levels were not altered, indicating that its availability does not seem to be the cause of hepatic oxidative stress. As a further indication of the impairment of the hepatic antioxidant defenses is the observation that catalase and SOD, which contribute to scavenge ROS, were both reduced by the MG treatment [55, 65]. In addition, SIRT1, whose hepatic expression was inhibited by MG, is reported to upregulate the expression of SOD and catalase [66]. Hepatic HO-1 expression was increased by MG, which may have both pro- and antioxidant effects. Its expression is, in fact, elevated in steatohepatitis as an adaptive response to oxidative stress [67].

### *Lipid metabolism and ketogenesis*

In the present study, MG did not modify the total lipid content in the liver and even decreased the hepatic content of TAG. This suggests that the administration of MG did not result in hepatic steatosis but in increased catabolism linked to high-grade inflammation and cirrhosis [15, 20]. Rats that received MG present lower body weight gain without diminishing the total fat mass, i.e., there is loss of lean mass [22, 24]. The reason for the lower body weight gain is not solely anorexia, but metabolic alterations due to systemic inflammation are also partly responsible [68, 69]. Corroborating this conclusion is our observation that rats that received MG at a lower dose (25 mg/kg) had a lower weight gain without reduction of food intake.

MG did not change the total fat mass of rats, but it modified the pattern of body visceral fat depots. In the mesenteric tissue, the fat mass and the area of adipocytes increased while the opposite occurred in the periepididymal and retroperitoneal tissues. It is true that the fat mass of young rats (~60 days old) is still very low (~3% of body weight) when compared to adult rats [70] and there is no certainty that this modified distribution will be maintained along the entire life period. On the other hand, the expression and activation of the AMPK protein is consistent phenomenon. The AMPK protein, known to stimulate lipolysis in adipose tissue, had its expression reduced in the mesenteric tissue while both expression and activation (p-AMPK) were increased in the retroperitoneal adipose tissue of fasted rats that received MG. In fact, the retroperitoneal fat depot has higher capacity to release fatty acids compared to the mesenteric fat depot and AMPK can be differently regulated in different tissues, being even able to stimulate or inhibit lipolysis in adipose tissue [71, 72]. The higher levels of glycerol found in plasma of fasted rats that received MG corroborate a stimulated lipolysis in the adipose tissue, particularly in the retroperitoneal fat tissue, and also indicate

higher circulating levels of free fatty acids (FFA). This should cause an increased influx of FFA to the liver. The breakdown of FFA into ketone bodies and the palmitate-dependent extra oxygen uptake were increased in the livers of rats that received MG, two observations that are consistent with the hypothesis. It is also worth to mention that systemic inflammation is associated with a higher hepatic FFA uptake and oxidation [20].

The levels of TAG and ketone bodies were decreased in the plasma of fasted rats that received MG. The lower levels of hepatic and circulating TAG in these rats may have resulted from the increased FFA oxidation in the liver. Lower hepatic lipogenesis, an omnipresent event in advanced cirrhosis and high-grade systemic inflammation [20, 73], may also have contributed to the phenomenon. At this point it is important to note that the higher rate of ketogenesis described here for livers from fasted rats that received MG are in apparent contradiction to the lower levels of circulating ketone bodies found under this condition. However, this phenomenon has been reported for rats with high-grade systemic inflammation and there is evidence indicating that it occurs as a consequence of an increased uptake by peripheral tissues [20]. Ketone bodies are eagerly absorbed in the peripheral tissues by the monocarboxylate transporter 1 (MCT1), which is present in virtually every cell and is upregulated by cytokines in skeletal muscle [74, 75].

Rats that received MG presented a strongly modified glucose tolerance curve and insulin resistance. On this respect it has been claimed that the administration of MG to rats causes glucose intolerance, decreases the insulin-stimulated glucose uptake in adipose tissue and promotes pancreatic dysfunction [23]. In addition, insulin resistance is also an important hallmark in advanced cirrhosis [76]. However, rats that received MG presented lower fasting glycemia. This is a somewhat surprising result if one takes into account that insulin resistance is generally associated with high levels of blood glucose. The phenomenon is possibly the consequence of an excessive catabolism linked to the high-grade systemic inflammation and lower release of hepatic glucose. The latter can be the result of lower hepatic glycogen content associated with to lower gluconeogenesis in the rats that received MG.

#### *Gluconeogenesis and glycolysis*

The metabolic fluxes of carbohydrates in the liver were also modified by MG in a way that anabolic processes were diminished and catabolic fluxes were increased. In relation to anabolic process, MG inhibited gluconeogenesis from two precursors, namely lactate and glycerol. Two events seem to contribute to the phenomenon: a deficient energy supply from mitochondrial oxidative phosphorylation and a downregulation of gluconeogenic key enzymes. The reports on the effects of MG on the respiratory activity of isolated hepatic mitochondria show inconsistencies, as mitochondrial dysfunction and no alterations have been reported [77-79]. In the present study, isolated mitochondria were indeed affected by MG; specifically, the MMP was lower, and oxygen uptake was accelerated when succinate was the precursor. This shows an increased activity of the respiratory chain, more precisely a slight uncoupling action, but without pronounced reductions in ATP production. Thus, a deficient mitochondrial energy supply cannot be the main responsible for the impaired gluconeogenesis. In fact, glucose production from glycerol and lactate were equally impaired and glycerol gluconeogenesis needs only a third of the energy required for lactate gluconeogenesis.

With respect to the rate-limiting enzymes, MG decreased the activity and mRNA expression of both PEPCK and FBPase-1, and the activity of G6Pase. These are certainly key determinants in reducing hepatic gluconeogenesis. It has been shown that pro-inflammatory cytokines inhibit PEPCK expression in the liver and AGE are reported to increase the expression of the carbohydrate responsive element-binding protein (ChREBP), which decreases the expression of PEPCK in hepatic cells [80, 81]. In addition, pro-inflammatory cytokines and IL-1 $\beta$  have been shown to diminish hepatic alanine gluconeogenesis in healthy rats [82] and IL-6 has been shown to inhibit gluconeogenesis in the liver of healthy mice and to downregulate the expression of gluconeogenic key enzymes in the liver of mice with NASH and hepatocarcinogenesis [83, 84]. In turn, protein levels and phosphorylation of AMPK, known to downregulate gluconeogenesis, was not modified in the liver of rats that received

MG [72]. In this regard, AMPK has been reported not to be required for the downregulation of hepatic gluconeogenesis and, in addition, pro-inflammatory cytokines diminish AMPK expression and activation in the liver [72, 85].

The higher hepatic expression of G6Pase mRNA in rats that received MG is an apparently contradictory result if one considers that the activity of this enzyme was reduced. Because G6Pase is not covalently regulated, its activity, when measured under standard conditions, reflects its active protein level in the microsomal fraction. An explanation for the apparent discrepancy would be a negative post-transcriptional regulation of the protein expression, a dysfunctional enzyme or even an enzyme maintained in compartments to which glucose 6-phosphate has no access (regulation by translocation) [86]. In this regard, FFA and fatty acyl-CoA increase G6Pase mRNA in the rat liver [87], however, the G6Pase expression is reported to be regulated also at the post-transcriptional level, with the protein being structurally modified by MG [88]. Gluconeogenesis in the present study, however, was inferred from metabolic fluxes measured in perfused livers, a system that maintains the fine regulation in terms of substrate concentrations and allosteric effectors [40]. The perfused liver provides, no doubt, a more reliable system to infer about the actual metabolic fluxes in the liver than mRNA expression or enzyme activities [40].

In relation to catabolic processes, the MG administration increased the glycerol flux through glycolysis in perfused livers from fasted rats, as indicated by the increased lactate production, but it did not modify oxygen consumption. The latter observation means that little pyruvate, which is formed by the lactate dehydrogenase equilibrium, is oxidized intramitochondrially. This could be indicating some degree of impairment of the mitochondrial functions that justifies the increased lactate production and the lowered glucose production. Increased lactate production by MG was also observed in HepG2 cells, an effect that was accompanied by increased glucose uptake and enhanced expression of glycolytic enzymes [89]. The latter also occurs in high-grade systemic inflammation and advanced cirrhosis [90] possibly due to the fact that IL-6 upregulates glycolytic enzymes in the liver [91]. In livers from fed rats, on the contrary, glycolysis at the expense of endogenous glycogen was diminished by the MG. This was probably the consequence of diminished glycogen levels caused by the high-grade systemic inflammation [68, 92].

## Conclusion

The administration of MG to healthy rats during seven days causes high-grade systemic inflammation and mild liver damage. The metabolic changes are similar to diseases associated with a widespread catabolism in the body, particularly advanced hepatic cirrhosis: reduction of food intake, loss of lean mass, lower body weight gain and increased systemic oxidative stress. In addition, MG causes insulin resistance, however, associated with a lower fasting glycemia, which is a consequence of both an excessive catabolism and lower release of hepatic glucose. Metabolic fluxes in the liver were modified by MG in a way that anabolic processes, such as gluconeogenesis and glycogenesis were diminished, and catabolic fluxes, such as glycolysis, were increased in the organ. Two factors can contribute to this outcome, though in unequal proportions: a mild deficiency in energy supply from the mitochondria and a much more significant downregulation of gluconeogenic key enzymes. Lipid metabolism in the adipose tissue was modified in a way that AMPK-stimulated lipolysis was increased in the retroperitoneal fat depot, but not in the mesenteric fat depot. In addition, ketogenesis was increased and the content of TAG was decreased in the liver. To what degree the modifications in hepatic energy metabolism found in MG-exposed rats can be translated to patients with a high-grade inflammation and cirrhosis is uncertain. However, it is unlikely that the strong catabolic state induced by MG would not contribute in some way to the hepatic dysfunction in advanced liver diseases.

**Abbreviations:** AFU, arbitrary fluorescence units; AGE, advanced glycation end

products; ALT, alanine aminotransferase; AMPK, AMP-activated protein kinase; p-AMPK, phosphorylated AMPK; AST, aspartate aminotransferase; AUC, area under the curve; BSA, bovine serum albumin; CML, carboxymethyl lysine; CHOL, cholesterol; DMSO, dimethyl sulfoxide; FBPase-1, fructose 1, 6-biphosphatase; FFA, free fatty acids; FRAP, ferric reduction capacity of plasma; G6Pase, glucose 6-phosphatase; GADPH, glyceraldehyde-3-phosphate dehydrogenase; GPDH, glycerol-3-phosphate dehydrogenase; GK, glycerol kinase; GLO-I, glyoxalase I; GLO-II, glyoxalase II; GR, glutathione reductase; GPx1, glutathione peroxidase-1; GSH, reduced glutathione; GSSG, oxidized glutathione; GSTA3, glutathione S-transferase alpha 3; HO-1, heme oxygenase 1; IL-1, interleukin 1; IL-6, interleukin 6; ITT, insulin tolerance test; kITT, rate constant for insulin tolerance test; MG, methylglyoxal; MG-H1, methylglyoxal-derived hydroimidazolone 1; MMP, mitochondrial membrane potential; MMS, methanesulfonate; MPO, myeloperoxidase; MTT, 3-(4, 5-dimethylthiazol-2-yl)-2, 5-diphenyl tetrazolium bromide; NAFLD, non-alcoholic fatty liver disease; NASH, nonalcoholic steatohepatitis; NF- $\kappa$ B, nuclear factor-kappa B; OGTT, oral glucose tolerance test; PBS, phosphate-buffered saline; PEPCK, phosphoenolpyruvate carboxykinase; RAGE, AGE receptor; RC, respiratory control; ROS, reactive oxygen species; SIRT1, sirtuin 1; SOD, superoxide dismutase; TAC, total antioxidant capacity; TAG, triacylglycerol; TNF- $\alpha$ , tumoral necrosis factor alpha.

## Acknowledgements

The authors wish to thank the financial support of the Coordenação de Aperfeiçoamento de Pessoal de Nível Superior (CAPES) and Conselho Nacional de Desenvolvimento Científico e Tecnológico (CNPq). Naiara Cristina Lucredi thanks the funding by CAPES (process-88881.624409/2021-01) for the national financial support and incentive to research. The authors are grateful to the Mayo Clinics and Foundation (Florida, EUA) for financial support through the Helen Diller Family Foundation, the Glenn Foundation for Medical Research via the Paul F. Glenn Laboratories for the Biology of Aging, Calico Life Sciences LLC, National Institute on Aging Grants AG-26094 and AG58812, and National Cancer Institute Grant CA233790.

## Disclosure Statement

The authors have no conflicts of interest to declare.

## References

- 1 Brings S, Fleming T, Freichel M, Muckenthaler M, Herzig S, Nawroth P: Dicarbonyls and advanced glycation end-products in the development of diabetic complications and targets for intervention. *Int J Mol Sci* 2017;18:984. <https://doi.org/10.3390/ijms18050984>
- 2 Kalapos MP: Where does plasma methylglyoxal originate from? *Diabetes Res Clin Pract* 2013;99:260–271. <https://doi.org/10.1016/j.diabres.2012.11.003>
- 3 Rabbani N, Thornalley PJ: The critical role of methylglyoxal and glyoxalase 1 in diabetic nephropathy. *Diabetes* 2014;63:50–52. <https://doi.org/10.2337/db13-1606>
- 4 Schalkwijk CG, Stehouwer CDA: Methylglyoxal, a highly reactive dicarbonyl compound, in diabetes, its vascular complications, and other age-related diseases. *Physiol Rev* 2020;100:407-461. <https://doi.org/10.1152/physrev.00001.2019>
- 5 Thornalley PJ: The glyoxalase system: new developments towards functional characterization of a metabolic pathway fundamental to biological life. *Biochem J* 1990;269:1–11. <https://doi.org/10.1042/bj2690001>
- 6 Matafome P, Rodrigues T, Sena C, Seica R: Methylglyoxal in metabolic disorders: facts, myths, and promises. *Med Res Rev* 2016;37:368–403. <https://doi.org/10.1002/med.21410>

- 7 Tanaka N, Yonekura H, Yamagishi S, Fujimori H, Yamamoto Y, Yamamoto H: The receptor for advanced glycation end products is induced by the glycation products themselves and tumor necrosis factor- $\alpha$  through nuclear factor- $\kappa$ B, and by 17- $\beta$ -estradiol through Sp-1 in human vascular endothelial cells. *J Biol Chem* 2000;275:25781-25790. <https://doi.org/10.1074/jbc.M001235200>
- 8 Guilbaud A, Niquet-Leridon C, Boulanger E, Tessier F: How can diet affect the accumulation of advanced glycation end-products in the human body? *Foods* 2016;5:84. <https://doi.org/10.3390/foods5040084>
- 9 Smedsrød B, Melkko J, Araki N, Sano H, Horiuchi S: Advanced glycation end products are eliminated by scavenger-receptor-mediated endocytosis in hepatic sinusoidal Kupffer and endothelial cells. *Biochem J* 1997;322:567-573. <https://doi.org/10.1042/bj3220567>
- 10 Neves C, Rodrigues T, Sereno J, Simões C, Castelhana J, Gonçalves J, Bento G, Gonçalves S, Seça R, Domingues MR, Castelo-Branco M, Matafome P: Dietary glycotoxins impair hepatic lipidemic profile in diet-induced obese rats causing hepatic oxidative stress and insulin resistance. *Oxid Med Cell Longev* 2019;2019:6362910. <https://doi.org/10.1155/2019/6362910>
- 11 Bijnen M, van Greevenbroek MMJ, van der Kallen CJH, Scheijen JL, van der Waarenburg MPH, Stehouwer CDA, Wouters K, Schalkwijk CG: Hepatic fat content and liver enzymes are associated with circulating free and protein-bound advanced glycation end products, which are associated with low-grade inflammation: The CODAM study. *J Diabetes Res* 2019;2019:6289831. <https://doi.org/10.1155/2019/6289831>
- 12 Yang M, Fan J, Zhang J, Du J, Peng X: Visualization of methylglyoxal in living cells and diabetic mice model with a 1, 8-naphthalimide-based two-photon fluorescent probe. *Chem Sci* 2018;9:6758-6764. <https://doi.org/10.1039/c8sc02578a>
- 13 Wang W-C, Chou C-K, Chuang M-C, Li Y-C, Lee J-A: Elevated levels of liver methylglyoxal and d-lactate in early-stage hepatitis in rats. *Biomed Chromatogr* 2017;32:e4039. <https://doi.org/10.1002/bmc.4039>
- 14 Reddy JK, Rao MS: Lipid metabolism and liver inflammation. II. Fatty liver disease and fatty acid oxidation. *Am J Physiol Gastrointest Liver Physiol* 2006;290:G852-G858. <https://doi.org/10.1152/ajpgi.00521.2005>
- 15 Arakawa Y, Moriyama M, Arakawa Y: Liver cirrhosis and metabolism (sugar, protein, fat and trace elements). *Hepatol Res* 2004;30S:46-58. <https://doi.org/10.1016/j.hepres.2004.10.009>
- 16 Schauder P: Catabolism in patients with liver cirrhosis; in: Müller MJ, Danforth E, Burger AG, Siedentopp U (eds): *Hormones and Nutrition in Obesity and Cachexia*. Springer, Berlin, Heidelberg, 1990, pp 95-103. [https://doi.org/10.1007/978-3-642-75037-3\\_10](https://doi.org/10.1007/978-3-642-75037-3_10)
- 17 Michel M, Hess C, Kaps L, Kremer WM, Hilscher M, Galle PR, Moehler M, Schattenberg JM, Wörns MA, Labenz C, Nagel M: Elevated serum levels of methylglyoxal are associated with impaired liver function in patients with liver cirrhosis. *Sci Rep* 2021;11:20506. <https://doi.org/10.1038/s41598-021-00119-7>
- 18 Arroyo V, Angeli P, Moreau R, Jalan R, Clària J, Trebicka J, Fernández J, Gustot T, Caraceni P, Bernardi M: The systemic inflammation hypothesis: Towards a new paradigm of acute decompensation and multiorgan failure in cirrhosis. *J Hepatol* 2021;74:670-685. <https://doi.org/10.1016/j.jhep.2020.11.048>
- 19 Engelmann C, Clària J, Szabo G, Bosch J, Bernardi M: Pathophysiology of decompensated cirrhosis: Portal hypertension, circulatory dysfunction, inflammation, metabolism and mitochondrial dysfunction. *J Hepatol* 2021;75:S49-S66. <https://doi.org/10.1016/j.jhep.2021.01.002>
- 20 Wendt MMN, de Oliveira MC, Franco-Salla GB, Castro LS, Parizotto AV, Souza-Silva FM, Natali MRM, Bersani-Amado CA, Bracht A, Comar JF: Fatty acids uptake and oxidation are increased in the liver of rats with adjuvant-induced arthritis. *Biochim Biophys Acta Mol Basis Dis* 2019;1865:696-707. <https://doi.org/10.1016/j.bbadis.2018.12.019>
- 21 Van Wyngene L, Vandewalle J, Libert C: Reprogramming of basic metabolic pathways in microbial sepsis: therapeutic targets at last? *EMBO Mol Med* 2018;10:e8712. <https://doi.org/10.15252/emmm.201708712>
- 22 Sena CM, Matafome P, Crisóstomo J, Rodrigues L, Fernandes R, Pereira P, Seça RM: Methylglyoxal promotes oxidative stress and endothelial dysfunction. *Pharmacol Res* 2012;65:497-506. <https://doi.org/10.1016/j.phrs.2012.03.004>
- 23 Dhar A, Desai KM, Wu L: Alagebrium attenuates acute methylglyoxal-induced glucose intolerance in Sprague-Dawley rats. *Br J Pharmacol* 2010;159:166-175. <https://doi.org/10.1111/j.1476-5381.2009.00469.x>
- 24 Yang SE, Lin YF, Liao JW, Chen JT, Chen CL, Chen CI, Hsu SL, Song TY: Insulin sensitizer and antihyperlipidemic effects of *Cajanus cajan* (L.) millsp. root in methylglyoxal-induced diabetic rats. *Chin J Physiol* 2022;65:125-135. [https://doi.org/10.4103/cjp.cjp\\_88\\_21](https://doi.org/10.4103/cjp.cjp_88_21)

- 25 Ghosh M, Talukdar D, Ghosh S, Bhattacharyya N, Ray M, Ray S: *In vivo* assessment of toxicity and pharmacokinetics of methylglyoxal. Augmentation of the curative effect of methylglyoxal on cancer-bearing mice by ascorbic acid and creatine. *Toxicol Appl Pharmacol* 2006;212:45-58. <https://doi.org/10.1016/j.taap.2005.07.003>
- 26 Cat AND, Briones AM: Isolation of mature adipocytes from white adipose tissue and gene expression studies by real-time quantitative RT-PCR. *Methods Mol Biol* 2017;1527:283-295. [https://doi.org/10.1007/978-1-4939-6625-7\\_22](https://doi.org/10.1007/978-1-4939-6625-7_22)
- 27 Bradley PP, Christensen RD, Rothstein G: Cellular and extracellular myeloperoxidase in pyogenic inflammation. *Blood* 1982;60:618-622. <https://doi.org/10.1182/blood.V60.3.618.618>
- 28 Davidson MB, Karjala R: Simplified fluorometric method for the determination of plasma glycerol. *J Lipid Res* 1970;11:609-612. [https://doi.org/10.1016/S0022-2275\(20\)42946-3](https://doi.org/10.1016/S0022-2275(20)42946-3)
- 29 Bergmeyer HU: *Methods of Enzymatic Analysis*, London: Verlag Chemie-Academic Press, 1974. ISBN: 352725370X, 9783527253708
- 30 Lobo Jr JP, Brescansin CP, Santos-Weiss ICR, Welter M, Souza EM, Rego FGM, Picheth G, Alberton D: Serum fluorescent advanced glycation end (F-AGE) products in gestational diabetes patients. *Arch Endocrinol Metab* 2017;61:233-237. <https://doi.org/10.1590/2359-3997000000238>
- 31 Benzie IFF, Strain JJ: The ferric reducing ability of plasma (FRAP) as a measure of "antioxidant power": the FRAP assay. *Anal Biochem* 1996;239:70-76. <https://doi.org/10.1006/abio.1996.0292>
- 32 Bracht A, Silveira SS, Castro-Ghizoni CV, Sá-Nakanishi AB, Oliveira MRN, Bersani-Amado CA, Peralta RM, Comar JF: Oxidative changes in the blood and serum albumin differentiate rats with monoarthritis and polyarthritis. *SpringerPlus* 2016;5:36-50. <https://doi.org/10.1186/s40064-016-1671-1>
- 33 Levine RL, Garland D, Oliver CN, Amici A, Climent I, Lenz AG, Ahn BW, Shaltiel S, Stadtman ER: Determination of carbonyl content in oxidatively modified proteins. *Methods Enzymol* 1990;186:464-478. [https://doi.org/10.1016/0076-6879\(90\)86141-h](https://doi.org/10.1016/0076-6879(90)86141-h)
- 34 Hissin PJ, Hilf R: Fluorimetric method for determination of oxidized and reduced glutathione in tissues. *Analyt Biochem* 1976;74:214-226. [https://doi.org/10.1016/0003-2697\(76\)90326-2](https://doi.org/10.1016/0003-2697(76)90326-2)
- 35 Biazon ACB, Wendt MMN, Moreira JR, Castro-Ghizoni CV, Soares AA, Silveira SS, Sa-Nakanishi AB, Bersani-Amado CA, Peralta RM, Bracht A, Comar JF: The *in vitro* antioxidant capacities of hydroalcoholic extracts from roots and leaves of *Smilax sonchifolius* (yacon) do not correlate with their *in vivo* antioxidant action in diabetic rats. *J Biosci Med* 2016;4:15-27. <https://doi.org/10.4236/jbm.2016.42003>
- 36 Marklund S, Marklund G: Involvement of the superoxide anion radical in the oxidation of pyrogallol and a convenient assay for superoxide dismutase. *Eur J Biochem* 1974;47:469-474. <https://doi.org/10.1111/j.1432-1033.1974.tb03714.x>
- 37 Comar JF, Suzuki-Kemmelmeier F, Bracht A: The action of oxybutinin on haemodynamics and metabolism in the perfused rat liver. *Basic Clin Pharmacol Toxicol* 2003;93:147-152. <https://doi.org/10.1034/j.1600-0773.2003.930307.x>
- 38 Simões M, Ames-Sibin AP, Lima EP, Pateis VO, Bersani-Amado CA, Mathias PCF, Peralta RM, Sá-Nakanishi AB, Bracht L, Bracht A, Comar JF: Resveratrol biotransformation and actions on the liver metabolism of healthy and arthritic rats. *Life Sci* 2022;310:120991. <https://doi.org/10.1016/j.lfs.2022.120991>
- 39 Oliveira AL, Comar JF, de Sá-Nakanishi AB, Peralta RM, Bracht A: The action of p-synephrine on hepatic carbohydrate metabolism and respiration occurs via both Ca(2+)-mobilization and cAMP production. *Mol Cell Biochem* 2014;388:135-147. <https://doi.org/10.1007/s11010-013-1905-2>
- 40 Sá-Nakanishi AB, de Oliveira MC, Pateis VO, Silva LAP, Pereira-Maróstica HV, Gonçalves GA, Oliveira MAS, Godinho J, Bracht L, Milani H, Bracht A, Comar JF: Glycemic homeostasis and hepatic metabolism are modified in rats with global cerebral ischemia. *Biochim Biophys Acta Mol Basis Dis* 2020;1866:165934. <https://doi.org/10.1016/j.bbadis.2020.165934>
- 41 Lima LC, Buss GD, Ishii-Iwamoto EL, Salgueiro-Pagadigorria CL, Comar JF, Bracht A, Constantin J: Metabolic effects of p-coumaric acid in the perfused rat liver. *J Biochem Mol Toxicol* 2006;20:18-26. <https://doi.org/10.1002/jbt.20114>
- 42 Vilela VR, Oliveira AL, Comar JF, Peralta RM, Bracht A: Effects of tadalafil on the cAMP stimulated glucose output in the rat liver. *Chem Biol Interact* 2014;220:1-11. <https://doi.org/10.1016/j.cbi.2014.05.020>
- 43 Souza KS, Moreira LS, Silva BT, Oliveira BPM, Carvalho AS, Silva PS, Verri WA Jr, Sá-Nakanishi AB, Bracht L, Zanoni JN, Gonçalves OH, Bracht A, Comar JF: Low dose of quercetin-loaded pectin/casein microparticles reduces the oxidative stress in arthritic rats. *Life Sci* 2021;284:119910. <https://doi.org/10.1016/j.lfs.2021.119910>

- 44 Sá-Nakanishi AB, Soni-Neto J, Moreira LS, Gonçalves GA, Silva-Comar FMS, Bracht L, Bersani-Amado CA, Peralta RM, Bracht A, Comar JF: Anti-inflammatory and antioxidant actions of methyl jasmonate are associated with metabolic modifications in the liver of arthritic rats. *Oxid Med Cell Longev* 2018;2018:2056250. <https://doi.org/10.1155/2018/2056250>
- 45 Sá-Nakanishi AB, Soares AA, de Oliveira AL, Comar JF, Peralta RM, Bracht A: Effects of treating old rats with an aqueous *Agaricus blazei* extract on oxidative and functional parameters of the brain tissue and brain mitochondria. *Oxid Med Cell Longev* 2014;2014:563179. <https://doi.org/10.1155/2014/563179>
- 46 Lowry OH, Rosebrough NJ, Farr AL, Randall RJ: Protein measurement with the Folin phenol reagent. *J Biol Chem* 1951;193:265-275. [https://doi.org/10.1016/S0021-9258\(19\)52451-6](https://doi.org/10.1016/S0021-9258(19)52451-6)
- 47 Mendonça DEA, Godoy MAF, Lucredi NC, Comar JF, Almeida IV, Vicentini VEP: Toxicogenic effects of the mushroom *Ganoderma lucidum* on human liver and kidney tumor cells and peripheral blood lymphocytes. *J Ethnopharmacol* 2023;307:116226. <https://doi.org/10.1016/j.jep.2023.116226>
- 48 Remor AP, de Matos FJ, Ghisoni K, da Silva TL, Eidt G, Búrigo M, de Bem AF, Silveira PC, de León A, Sanchez MC, Hohl A, Glaser V, Gonçalves CA, Quincozes-Santos A, Borba Rosa R, Latini A: Differential effects of insulin on peripheral diabetes-related changes in mitochondrial bioenergetics: involvement of advanced glycosylated end products. *Biochim Biophys Acta* 2011;1812:1460-1471. <https://doi.org/10.1016/j.bbadis.2011.06.017>
- 49 Mosmann T: Rapid colorimetric assay for cellular growth and survival: application to proliferation and cytotoxicity assays. *J Immunol Methods* 1983;65:55-63. [https://doi.org/10.1016/0022-1759\(83\)90303-4](https://doi.org/10.1016/0022-1759(83)90303-4)
- 50 Mukherjee S, Das S, Bedi M, Vadupu L, Ball WB, Ghosh A: Methylglyoxal-mediated Gpd1 activation restores the mitochondrial defects in a yeast model of mitochondrial DNA depletion syndrome. *Biochim Biophys Acta Gen Subj* 2023;1867:130328. <https://doi.org/10.1016/j.bbagen.2023.130328>
- 51 Comar JF, de Oliveira DS, Bracht L, Kemmelmeier FS, Peralta RM, Bracht A: The Metabolic responses to l-glutamine of livers from rats with diabetes types 1 and 2. *PLoS One* 2016;11:e0160067. <https://doi.org/10.1371/journal.pone.0160067>
- 52 Viollet B, Foretz M, Guigas B, Horman S, Dentin R, Bertrand L, Hue L, Andreelli F: Activation of AMP-activated protein kinase in the liver: a new strategy for the management of metabolic hepatic disorders. *J Physiol* 2006;574:41-53. <https://doi.org/10.1113/jphysiol.2006.108506>
- 53 Patel R, Baker SS, Liu W, Desai S, Alkhoury R, Kozielski R, Mastrandrea L, Sarfraz A, Cai W, Vlassara H, Patel MS, Baker RD, Zhu L: Effect of dietary advanced glycation end products on mouse liver. *PLoS One* 2012;7:e35143. <https://doi.org/10.1371/journal.pone.0035143>
- 54 Pratt DS, Kaplan MM: Evaluation of abnormal liver-enzyme results in asymptomatic patients. *N Engl J Med* 2000;342:1266-1271. <https://doi.org/10.1056/NEJM200004273421707>
- 55 Comar JF, Sá-Nakanishi AB, de Oliveira AL, Wendt MMN, Bersani-Amado CA, Ishii-Iwamoto EL, Peralta RM, Bracht A: Oxidative state of the liver of rats with adjuvant-induced arthritis. *Free Rad Biol Med* 2013;58:144-53. <https://doi.org/10.1016/j.freeradbiomed.2012.12.003>
- 56 Moreira LS, Chagas AC, Ames-Sibin AP, Pateis VO, Gonçalves OH, Silva-Comar FMS, Hernandez L, Sá-Nakanishi AB, Bracht L, Bersani-Amado CA, Bracht A, Comar JF: Alpha-tocopherol-loaded polycaprolactone nanoparticles improve the inflammation and systemic oxidative stress of arthritic rats. *J Tradit Complement Med* 2021;12:414-425. <https://doi.org/10.1016/j.jtcme.2021.12.003>
- 57 Wendt MM, Sá-Nakanishi AB, Castro-Ghizoni CV, Bersani-Amado CA, Peralta RM, Bracht A, Comar JF: Oxidative state and oxidative metabolism in the brain of rats with adjuvant-induced arthritis. *Exp Mol Pathol* 2015;98:549-57. <https://doi.org/10.1016/j.yexmp.2015.04.002>
- 58 Schubert AC, Wendt MM, Sá-Nakanishi AB, Bersani-Amado CA, Peralta RM, Comar JF, Bracht A: Oxidative state and oxidative metabolism of the heart from rats with adjuvant-induced arthritis. *Exp Mol Pathol* 2016;100:393-401. <https://doi.org/10.1016/j.yexmp.2016.03.005>
- 59 Kong X, Ma MZ, Huang K, Qin L, Zhang HM, Yang Z, Li XY, Su Q: Increased plasma levels of the methylglyoxal in patients with newly diagnosed type 2 diabetes 2. *J Diabetes* 2014;6:535-540. <https://doi.org/10.1111/1753-0407.12160>
- 60 Wang WC, Chou CK, Chuang MC, Li YC, Lee JA: Elevated levels of liver methylglyoxal and d-lactate in early-stage hepatitis in rats. *Biomed Chromatogr* 2018;32:10.1002/bmc.4039. <https://doi.org/10.1002/bmc.4039>
- 61 Rabbani N, Thornalley PJ: Glyoxalase 1 Modulation in Obesity and Diabetes. *Antioxid Redox Signal* 2019;30:354-374. <https://doi.org/10.1089/ars.2017.7424>

- 62 Bhattacharyya N, Pal A, Patra S, Haldar AK, Roy S, Ray M: Activation of macrophages and lymphocytes by methylglyoxal against tumor cells in the host. *Int Immunopharmacol* 2008;8:1503-1512. <https://doi.org/10.1016/j.intimp.2008.06.005>
- 63 Ramasamy R, Vannucci SJ, Yan SS, Herold K, Yan SF, Schmidt AM: Advanced glycation end products and RAGE: a common thread in aging, diabetes, neurodegeneration, and inflammation. *Glycobiology* 2005;15:16R-28R. <https://doi.org/10.1093/glycob/cwi053>
- 64 Zhao W, Xu W, Jiang H: Relevance of SIRT1-NF- $\kappa$ B axis as therapeutic target to ameliorate inflammation in liver disease. *Int J Mol Sci* 2020;21:9460. <https://doi.org/10.3390/ijms21249460>
- 65 Choudhary D, Chandra D, Kale RK: Influence of methylglyoxal on antioxidant enzymes and oxidative damage. *Toxicol Lett* 1997;93:141-152. [https://doi.org/10.1016/s0378-4274\(97\)00087-8](https://doi.org/10.1016/s0378-4274(97)00087-8)
- 66 Alqrad MAI, El-Agamy DS, Ibrahim SRM, Sirwi A, Abdallah HM, Abdel-Sattar E, El-Halawany AM, Elsaed WM, Mohamed GA: SIRT1/Nrf2/NF- $\kappa$ B signaling mediates anti-inflammatory and anti-apoptotic activities of oleanolic acid in a mouse model of acute hepatorenal damage. *Medicina (Kaunas, Lithuania)* 2023;59:1351. <https://doi.org/10.3390/medicina59071351>
- 67 Malaguarnera L, Madeddu R, Palio E, Arena N, Malaguarnera M: Heme oxygenase-1 levels and oxidative stress-related parameters in non-alcoholic fatty liver disease patients. *J Hepatol* 2005;42:585-591. <https://doi.org/10.1016/j.jhep.2004.11.040>
- 68 Muscaritoli M, Imbimbo G, Jager-Wittenaar H, Cederholm T, Rothenberg E, di Girolamo FG, Amabile MI, Sealy M, Schneider S, Barazzoni R, Biolo G, Molino A: Disease-related malnutrition with inflammation and cachexia. *Clin Nutr* 2023;42:1475-1479. <https://doi.org/10.1016/j.clnu.2023.05.013>
- 69 Martín AI, Castellero E, Granado M, López-Menduiña M, Villanúa MA, López-Calderón A: Adipose tissue loss in adjuvant arthritis is associated with a decrease in lipogenesis, but not with an increase in lipolysis. *J Endocrinol* 2008;197:111-119. <https://doi.org/10.1677/JOE-07-0491>
- 70 DiGirolamo M, Fine JB, Tagra K, Rossmanith R: Qualitative regional differences in adipose tissue growth and cellularity in male Wistar rats fed ad libitum. *Am J Physiol* 1998;274:R1460-467. <https://doi.org/10.1152/ajpregu.1998.274.5.R1460>
- 71 Palou M, Sánchez J, Priego T, Rodríguez AM, Picó C, Palou A: Regional differences in the expression of genes involved in lipid metabolism in adipose tissue in response to short- and medium-term fasting and refeeding. *J Nutr Biochem* 2010;21:23-33. <https://doi.org/10.1016/j.jnutbio.2008.10.001>
- 72 Jeon SM: Regulation and function of AMPK in physiology and diseases. *Exp Mol Med* 2016;48:e245. <https://doi.org/10.1038/emm.2016.81>
- 73 Privitera G, Spadaro L, Marchisello S, Fede G, Purrello F: Abnormalities of lipoprotein levels in liver cirrhosis: Clinical relevance. *Dig Dis Sci* 2018;63:16-26. <https://doi.org/10.1007/s10620-017-4862-x>
- 74 Benton CR, Yoshida Y, Lally J, Han XX, Hatta H, Bonen A: PGC-1 $\alpha$  increases skeletal muscle lactate uptake by increasing the expression of MCT1 but not MCT2 or MCT4. *Physiol Genomics* 2008;35:45-54. <https://doi.org/10.1152/physiolgenomics.90217.2008>
- 75 Puigserver P, Rhee J, Lin J, Wu Z, Yoon JC, Zhang CY, Krauss S, Mootha VK, Lowell BB, Spiegelman BM: Cytokine stimulation of energy expenditure through p38 MAP kinase activation of PPAR $\gamma$  coactivator-1. *Mol Cell* 2001;8:971-982. [https://doi.org/10.1016/S1097-2765\(01\)00390-2](https://doi.org/10.1016/S1097-2765(01)00390-2)
- 76 Dietrich CG, Götte O, Geier A: Molecular changes in hepatic metabolism and transport in cirrhosis and their functional importance. *World J Gastroenterol* 2016;22:72-88. <https://doi.org/10.3748/wjg.v22.i1.72>
- 77 Seo K, Ki SH, Shin SM: Methylglyoxal induces mitochondrial dysfunction and cell death in liver. *Toxicol Res* 2014;30:193-198. <https://doi.org/10.5487/TR.2014.30.3.193>
- 78 Prestes AS, Dos Santos MM, Kamdem JP, Mancini G, Schüler da Silva LC, Bem AF, Barbosa NV: Methylglyoxal disrupts the functionality of rat liver mitochondria. *Chem Biol Interact* 2022;351:109677. <https://doi.org/10.1016/j.cbi.2021.109677>
- 79 Ghosh A, Bera S, Ghosal S, Ray S, Basu A, Ray M: Differential inhibition/inactivation of mitochondrial complex I implicates its alteration in malignant cells. *Biochemistry (Mosc)* 2011;76:1051-1060. <https://doi.org/10.1134/S0006297911090100>
- 80 Feingold KR, Moser A, Shigenaga JK, Grunfeld C: Inflammation inhibits the expression of phosphoenolpyruvate carboxykinase in liver and adipose tissue. *Innate Immun* 2012;18:231-240. <https://doi.org/10.1177/1753425911398678>
- 81 Chen H, Li Y, Zhu Y, Wu L, Meng J, Lin N, Yang D, Li M, Ding W, Tong X, Su Q: Advanced glycation end products promote ChREBP expression and cell proliferation in liver cancer cells by increasing reactive oxygen species. *Medicine (Baltimore)* 2017;96:e7456. <https://doi.org/10.1097/MD.00000000000007456>

- 82 Kelmer-Bracht AM, Broetto-Biazon AC, de Sá-Nakanishi AB, Ishii-Iwamoto EL, Bracht A: Low doses of tumour necrosis factor alpha and interleukin 1beta diminish hepatic gluconeogenesis from alanine *in vivo*. *Basic Clin Pharmacol Toxicol* 2006;99:335-339.
- 83 Wang B, Hsu SH, Frankel W, Ghoshal K, Jacob ST: Stat3-mediated activation of microRNA-23a suppresses gluconeogenesis in hepatocellular carcinoma by down-regulating glucose-6-phosphatase and peroxisome proliferator-activated receptor gamma, coactivator 1 alpha. *Hepatology* 2012;56:186-197. <https://doi.org/10.1002/hep.25632>
- 84 Inoue H, Ogawa W, Ozaki M, Haga S, Matsumoto M, Furukawa K, Hashimoto N, Kido Y, Mori T, Sakaue H, Teshigawara K, Jin S, Iguchi H, Hiramatsu R, LeRoith D, Takeda K, Akira S, Kasuga M: Role of STAT-3 in regulation of hepatic gluconeogenic genes and carbohydrate metabolism *in vivo*. *Nat Med* 2004;10:168-174. <https://doi.org/10.1038/nm980>
- 85 Johanns M, Hue L, Rider MH: AMPK inhibits liver gluconeogenesis: fact or fiction? *Biochem J* 2023;480:105-125. <https://doi.org/10.1042/BCJ20220582>
- 86 Stanton RC: Glucose-6-phosphate dehydrogenase, NADPH, and cell survival. *IUBMB Life* 2012;64:362-369. <https://doi.org/10.1002/iub.1017>
- 87 Van Schaftingen E, Gerin I: The glucose-6-phosphatase system. *Biochem J* 2002;362:513-532. <https://doi.org/10.1042/0264-6021:3620513>
- 88 Massillon D: Regulation of the glucose-6-phosphatase gene by glucose occurs by transcriptional and post-transcriptional mechanisms. Differential effect of glucose and xylitol. *J Biol Chem* 2001;276:4055-4062. <https://doi.org/10.1074/jbc.M007939200>
- 89 Sruthi CR, Raghu KG: Methylglyoxal induces ambience for cancer promotion in HepG2 cells via Warburg effect and promotes glycation. *J Cell Biochem* 2022;123:1532-1543. <https://doi.org/10.1002/jcb.30215>
- 90 Li J, Wang T, Xia J, Yao W, Huang F: Enzymatic and nonenzymatic protein acetylations control glycolysis process in liver diseases. *FASEB J* 2019;33:11640-11654. <https://doi.org/10.1096/fj.201901175R>
- 91 Soto-Herederó G, Gómez de Las Heras MM, Gabandé-Rodríguez E, Oller J, Mittelbrunn M: Glycolysis - a key player in the inflammatory response. *FEBS J* 2020;287:3350-3369. <https://doi.org/10.1111/febs.15327>
- 92 Castro-Ghizoni CV, Ames APA, Lameira OA, Bersani-Amado CA, Sá-Nakanishi AB, Bracht L, Marçal-Natali MR, Peralta RM, Bracht A, Comar JF: Anti-inflammatory and antioxidant actions of copaiba oil are related to liver cell modifications in arthritic rats. *J Cell Biochem* 2017;118:3409-3423. <https://doi.org/10.1002/jcb.25998>
- 93 Habeeb AF: Determination of free amino groups in proteins by trinitrobenzenesulfonic acid. *Anal Biochem* 1966;14:328-336. [https://doi.org/10.1016/0003-2697\(66\)90275-2](https://doi.org/10.1016/0003-2697(66)90275-2)